Hindawi
Mathematical Problems in Engineering
Volume 2022, Article ID 6955713, 20 pages
https://doi.org/10.1155/2022/6955713

Research Article

Cooperative Recharge Scheme Based on a Hamiltonian Path in Mobile Wireless Rechargeable Sensor Networks

He Li,[1,2] **Quan Liu**,[3] **Xiaopu Ma**,[3] **Qinglei Qi**,[1,2] **Jinjiang Liu**,[3] **Pan Zhao**,[4,5] **Yang Yang**,[2] **and Xingang Zhang**[1]

[1]*Henan Engineering Research Center of Intelligent Processing for Big Data of Digital Image, School of Computer Science and Technology, Nanyang Normal University, Nanyang 473061, China*
[2]*State Key Laboratory of Networking and Switching Technology, Beijing University of Posts and Telecommunications, Beijing 100876, China*
[3]*Institute for Research in Big Data Application, School of Computer Science and Technology, Nanyang Normal University, Nanyang 473061, China*
[4]*Key Laboratory of Grain Information Processing and Control (Henan University of Technology), Ministry of Education, Zhengzhou 450001, China*
[5]*Key Laboratory of Henan Province for Grain Photoelectric Detection and Control, Henan University of Technology, Zhengzhou 450001, China*

Correspondence should be addressed to Qinglei Qi; qingleiqi@126.com

Received 18 January 2022; Revised 23 March 2022; Accepted 29 March 2022; Published 19 May 2022

Academic Editor: Jun Li

The energy problem and limited capacity of batteries have been fundamental constraints in many wireless sensor network (WSN) applications. For WSN, the wireless energy transmission technology based on magnetic resonance coupling is a promising energy transmission technology. To reduce the cost and energy consumption during charging in mobile wireless rechargeable sensor networks (MWRSNs), a cooperative mobile charging mechanism based on the Hamiltonian path is proposed in this paper. To improve the charging task interval, we study the use of a mobile charger (MC) as a mobile sink node to collect the data in this paper. Then, we used the sink and the charging sensors selected by the MC to construct the undirected complete graph. Finally, the Euclidean distance between nodes is used as the edge weight and a Hamiltonian loop is found by using the improved Clark–Wright (C-W) saving algorithm to solve the problem of charging a rechargeable sensor network. In addition to the energy usage efficiency (EUE) and the network lifetime, the average energy loss per unit time is considered as the evaluation index according to the impact of the MC on the energy consumption during charging. The simulation results show that the proposed scheme increases the average network lifetime, decreases the average energy loss per unit time, and improves the EUE.

1. Introduction

WSNs have been applied in various monitoring applications, including ambient air monitoring [1], forest fire detection [2], electric networks [3], ecological environment monitoring [4], and medical health monitoring [5]. However, the energy requirement was not filled because of high computational resources, unreachable sensor nodes, and additional maintenances [6]. Kurs et al. [7] proposed a coupling resonance method to charge remote targets wirelessly with high efficiency and demonstrated the feasibility of wireless charging. The wireless energy transmission technology has the following advantages[8]:

- Charging and charged instruments do not need to be wired or connected
- Charging direction is not fixed and does not need to be in the visual range
- Compared with other environments, the method to obtain energy is predictable, stable, and controllable

With the increasing development of wireless energy transmission technology, research on wireless rechargeable sensor networks (WRSNs) is gradually increasing. Recently, WRSNs have been proposed, and multiple harvesting techniques can be used to charge the batteries of the rechargeable sensor nodes.

MWRSN is a mobile module added on the basis of WRSN, which attaches the MC and wireless sensor nodes to mobile objects. A mobile rechargeable sensor network refers to the active charging power node in a network, which can charge wireless nodes for rechargeable sensor nodes by moving. Compared with ordinary sensor networks, mobile rechargeable sensor networks have the following characteristics:

Rechargeability: the power of mobile rechargeable sensor nodes can be supplemented. In theory, the MWRSN can keep working permanently.

Mobility: the movement of the MC nodes and sensor nodes makes the topology of WSN change dynamically.

Limitation: in practical applications, the charging capacity of the MC is limited, which is reflected in the limited moving speed, charging power, and total energy.

Theoretically, the MWRSN can remain in permanent operation. However, in practical applications, the charging capacity of an MC is limited, which is manifested in limited moving speed, charging power, and total energy. Therefore, to realize the permanent existence of MWRSN, an MC is required not only to dynamically adjust its mobile charging mode according to the network state when charging task requests occur but also to cooperate with wireless sensor nodes to complete charging tasks efficiently.

At present, a number of studies have explored charging strategies and algorithms for MWRSN, most of which focused on offline recharging. Offline charging is assumed that the energy consumption rate of each sensor node is always fixed. The MC plans charging paths in advance according to the energy consumption of nodes in the network in the previous operation stage. During charging, MC moves along the planned paths periodically to replenish energy for sensor nodes [9]. However, in practice, the energy consumption rate of nodes is not fixed, and the energy consumption of sensor nodes shows high dynamics and diversity affected by the surrounding environment [10]. Therefore, if MC charges according to the predetermined charging path and strategy in offline charging, it will cause sensor node failure and serious degradation of the performance of the charging algorithm. To solve the problems of offline charging, some researchers put forward the online charging mechanism. In online charging, MC makes the charging strategy in real time and dynamically according to the actual residual energy of the sensor nodes. Compared with offline charging, online charging can better adapt to the energy needs and changes of actual nodes. However, the design of an online charging strategy has the following challenges:

Due to the dynamic change of node energy consumption rate, it is challenging to plan the charging path of MC dynamically in real time according to the actual remaining energy status of nodes and timely charge to avoid node failure.

The charging response should be fair. When the number of nodes requesting charging increases, the failure rate of sensor nodes should be reduced as much as possible.

In the charging process, the energy cost caused by MC movement should be reduced as much as possible and the energy carried by MC should be converted into effective energy for sensor charging as much as possible.

To solve these problems, in this paper, a stop-wait collaborative charging algorithm based on a Hamiltonian path is proposed in MWRSN. Compared with the existing work, the innovation of this paper is as follows:

To improve the charging task interval, we study the use of an MC as a mobile sink node to collect the data and establish the optimum model of the stop position.

To improve the EUE of MWRSN, the charging sensor node of the next round is considered as the current charging task scheduling in this algorithm when the power of MC is allowed.

To reduce the mobile path, an improved C-W saving algorithm is used to establish the Hamiltonian charging path according to the stop position of the mobile charger and the location of charging sensor nodes and sink.

To charge more sensors, the MC will not be fully charged for all sensors. As the MC passes by the stop-wait position, the stop-wait charging sensor node moves to meet with the MC and be charged.

2. Related Works

2.1. Optimization Schemes of the MWRSN. Rechargeable charging task scheduling problems for WSN have been studied in [9–15]. According to the wireless energy transmission technology, corresponding wireless sensor network models and optimization problems have been proposed. By solving the approximate optimal solution of the corresponding optimization problem, the charging scheme of the wireless charging node was obtained, which improves the charging efficiency of the sensor network. Budgetary constraints for different expenditure categories have been considered in [11]. The problem of scheduling the minimum number of MCs was investigated to replenish energy from all sensors in a WRSN. However, this method did not consider the dynamic topology problem when mobile charging nodes traverse sensor nodes in the network as data acquisition devices to collect data. A path planning model for mobile wireless charging equipment (WCE) based on multi-objective optimization was proposed to replenish energy and collect data in [12]. The limited energy of WCE in WRSN was considered to maximize the total energy utility of the mobile WCE and minimize the average delay of data transmission in this method. However, this method lacks

charging task coordination mechanism, which affected the charging utility and network energy consumption. To maximize the utilization rate of the MC and reduce the recharging delay, a cost-balanced mobile energy replenishment strategy (CBMERS) was proposed in [13]. According to their remaining lifetime, the nodes are assigned into groups to ensure that only nodes with lower residual energy in each slot are recharged. To balance the energy consumption between multiple MCs, the optimal trajectory allocation scheme was obtained by taking the moving distance and energy consumption as constraints. However, charging requests have an unbalanced effect on spatiotemporal constraints. To maximize the charging efficiency, a mixed-integer optimization model for simultaneous charging scheduling and charging time allocation is established in [14]. An offline algorithm was proposed to solve the problem, and an online charging node insertion algorithm was developed for real-time service. However, this method was only suitable for real-time business scenarios and not suitable for sparse networks. An efficient scheme for energy replenishment of sensor nodes was proposed to improve overall charging performance in [15]. The optimal trajectories for a given number of WCVs based on the routing loads of the sensor nodes were designed to make the network operational for a longer time. However, the rate of energy consumption varies dynamically due to the uncertainty of environmental conditions; therefore, a periodical charging scheme was infeasible for complex and changeable networks. In [16], a optimization problem with the target of maximizing the ratio of MC's vacation time over one entire cycle time is proposed to improve channel utilization and prolong network lifetime. However, this method did not involve the dynamic topology of WRSN. This method was not suitable for a mobile network with a dynamic topology. Then, an optimization problem was formulated to maximize the MC's vacation time over the rechargeable cycle. In [17], it was assumed that an MC must charge a sensor to its full energy capacity before moving to charge the next sensor and that each sensor could be partially charged. To maximize the sum of the sensor lifetimes and to minimize the travel distance of the MC, two novel optimization problems of scheduling an MC to charge a set of sensors were formulated. Although this method increases the number of nodes that an MC can serve, it also accelerates the scheduling frequency as well as the energy consumption rate of the MC.

A power beacon (PB) and multiple wireless powered user nodes were considered static networks in [18]. All user nodes assumed either a charge or work mode. A charge scheduling scheme that achieved the system's maximal energy efficiency was proposed, and this scheme was extended to a two-tier network architecture. An energy-efficient traveling path for multiple MCs was designed in [19]. This method divided the whole network into many subregions to maximize the benefit of multiple MCs. To find the charging points, the charging radius based nearest neighbor approach was used to improve the charging efficiency. However, different sensors have different contributions in terms of the monitoring quality that was ignored in this method. Similar to the study in [19], a novel fuzzy logic-based on-demand charging scheduling scheme in WRSNs [20] was proposed to equally distribute the workload to each MC. To recharge the nodes with different energy consumption rates, the adaptive threshold for charging requests was considered in this study. To prolong the life of WSN and minimize the travel distance of mobile chargers, a dynamic mobile charger scheduling (DPMCS) scheme is proposed in the literature [21]. The node requests a charge before it runs out of energy and the mobile charger charges it. This scheme uses deep reinforcement learning to determine the schedule of the mobile charger. It prolongs the life of WSN by reducing the number of dead zone nodes and minimizing the travel distance of the mobile charger. To maximize the network lifetime, a two-phase lifetime-enhancing method (TLM) is proposed in [22]. In the first phase, a multiobjective particle swarm optimization (MOPSO) algorithm was proposed to relocate useful mobile rechargeable sensor nodes at optimal locations to meet the full target coverage. In the second phase, a modified binary multiobjective evolutionary algorithm was adopted to extend the network lifetime. However, these methods did not consider the dynamic topology of an MC as a data acquisition device. In [23–26], an MC was considered a data collection device to obtain data information from the sensor node when charging the sensor node. Based on this concept, dynamic topology working modes in WRSN were proposed. However, these methods lacked the coordination mechanism of charging task, which affected the charging utility and network energy consumption.

2.2. Cooperative Schemes of the MWRSN. Energy efficiency remains a great challenge without collaboration. To increase the survival rate of nodes in 3D underwater networks, a new temporal and spatial collaborative charging algorithm with multiple mobile charging ships and charging stations (mCS-TS) was proposed in [27]. A concept of secondary charging stations for mobile charging ships was designed to reduce the traveling cost and improve charging efficiency. Simulation results show the effectiveness of the proposed algorithm. This method has the problem of spatiotemporal synchronization and lacks the cooperative collection mechanism of MC. The application of this method has certain scenario limitations.

The collaborative feature by forming a hierarchical charging structure was proposed in [28]. The authors distinguish the chargers into two groups: the hierarchically lower MCs which charge sensor nodes and the hierarchically higher special chargers (SCs) which charge MCs. Four collaborative charging protocols were proposed to achieve efficient charging and improve important network properties. However, this method does not consider the mobility of nodes and the dynamic changes in network topology. It will cause long moving paths and excessive energy consumption during the next cycle of task coordination.

To solve the periodic charging of WSN, in [29], the charging problem in WSN was modeled as a routing problem of mobile charging nodes with time windows. This method transformed multiple routing problems into a single routing problem and proposed a local optimization

algorithm considering the collaboration between mobile charging nodes. Simulation results showed that the proposed algorithm had certain advantages in charging scheduling. However, this method did not consider the dynamic topology of an MC as a data acquisition device when traversing sensor nodes in the network. In [30], a collaborative scheduling algorithm was proposed for mobile charging tasks, which allowed energy transfer between MCs. It was demonstrated that this algorithm could cover an infinite length of a one-dimensional (1D) wireless sensor network under three assumptions. Then, the hypothesis was removed one by one, and the method was extended to constrained two-dimensional (2D) wireless sensor network scenarios. Simulation results showed that this method could improve the energy efficiency of charging. This method lacks the cooperative collection mechanism of MC, resulting in the problems of short network lifetime and frequent charging task scheduling. To reduce costs, a novel concept and an optimal charging algorithm were introduced in [31]. It was demonstrated that push-shuttle-back (PSB) could achieve the minimum number of chargers and the optimal shuttling distance in a 1D scenario with negligible energy loss. The algorithm extended the solution to 2D scenarios and introduced a new circle-based scheme to improve charging efficiency and reduce the number of chargers needed to serve the sensor network. However, this method incurs high overhead; the major drawback is the large traveling cost because the MC needs to go back and forth between a charging station and sensors. To adapt to large-scale WRSN, a temporal-spatial charging scheduling algorithm was developed in [32]. This method aimed to minimize the number of dead nodes while maximizing energy efficiency to prolong the network lifetime. A node deletion algorithm was developed to remove low-efficiency charging nodes. Simulation results showed that this scheme could achieve promising performance in charging throughput and efficiency. However, this method fails to take into account the heterogeneous energy consumption of the nodes which should be given further consideration since it reduces the EUE. In [33], according to the importance of the sensor node (associated with the distance to the base station), the sensor nodes were divided into two types: sensor nodes in ring 0 and sensor nodes in the outer ring. To improve the charging efficiency, a novel charging model for wireless charging vehicles (WCVs) was proposed to adopt different charging strategies for different sensor nodes. To estimate the lifetime of the network, a new metric named the normalized dead time was proposed. The simulation results indicated that the performance of the WRSN could be improved. Due to the limited energy resources of WRSNs, there will be resource competition among nodes.

The limitations of these algorithms need to further study the collaborative charging scheduling problem of the MWRSN. In this work, a stop-wait collaborative charging algorithm is designed to improve the EUE of WSN. The charging sensor node of the next round is considered as the current charging task scheduling. The charging task interval of the MC is used to select the sensors and determine the charging sequence and stop-wait charging set. The position nearest to the stop-wait charging sensor node is selected as the stop-wait position. As the MC passes by the stop-wait position, the stop-wait charging sensor node moves to meet with the MC and be charged. To charge more sensors, the MC will not be fully charged for all sensors in our algorithm. The simulation results show that the stop-wait algorithm can achieve a better EUE of WSN compared with DPMCS [21], MUC [34], BNRS [35], and VN-MOAC [36] algorithms. Compared with existing cooperative mobile recharge schemes, our proposed algorithm contributes the following improvements:

- Considering the data collection of the MC, we first present a novel optimal approach to determine the stop position for the MC to collect data as a mobile sink node after the charging scheduling task is completed. Hence, the charging task interval can be extended.
- Then, a cooperative recharge scheme based on a Hamiltonian path is designed which utilizes the improved C-W method for determining the charging of the nodes by contemplating various network attributes.
- The charging sensor node of the next round is proposed as the stop-wait charging sensor node of the current round. The aim is to avoid the MC having to charge these nodes in the next round and reduce network energy consumption.
- Considering the limited power of the MC in the establishment of a mobile path, an incomplete charging mode is proposed to improve the serviceability of the MC. The sensor node is charged according to the maximum number of cycles that can be achieved between charging tasks.
- The proposed algorithm is evaluated through extensive simulations and compared with four existing and similar works in terms of EUE, average energy loss per unit time, and average network lifetime.

This paper is organized as follows: Section 2 presents brief related works of charging schemes. Section 3 introduces the assumptions, definitions, wireless rechargeable sensor network model, and network energy consumption model. Section 4 describes the algorithm of cooperative recharging based on the Hamiltonian path in the MWRSN. Simulation results and analyses of the algorithms are presented in Section 5. Finally, the conclusions are drawn in Section 6.

3. System Model

3.1. WSN Charging Model. Assume $S = \{s_i$, where i in $1, 2, \ldots, n\}$ is the senor node set of WSN, and the location of mobile wireless sensor node s_i is $l_i = (x_i, y_i)$. The communication radius of sensor s_i is r_i, and the average moving velocity of sensor s_i is v_i. The energy consumption of each sensor includes the energy consumption of data transmission and the movement of sensor nodes. The battery capacity of s_i is b_i, and the average energy consumption rate of s_i is e_i. The energy consumed by the sensor moving one unit distance is $e_{m,i}$. The maximum lifetime of s_i is τ_i and $\tau_i = b_i/e_i$. The

charge cycles of sensor s_i are $\tau_{c,i}$ and $\tau_{c,i} = b_i(1-\omega)/e_i$, where ω is the low power indicator percentage of the sensor to guarantee the normal work of sensor s_i. The MC will recharge sensor s_i when the power is less than $b_i\omega$. Assume that a low-power indicator percentage ω can ensure the remaining survival time of sensor node $b_i\omega/e_i$ and will not fail due to battery drainage before the MC task scheduling.

The battery capacity of the MC is B_C, and the average moving velocity of the MC is v_c. The movement and wireless charging of the MC share a battery charge, and the energy consumption of moving per unit distance for the MC is e_c. The sink node in this model serves as the base station data service point as well as the energy source. Without loss of generality, the sink is taken as the coordinate origin (0, 0). The MC starts to move from the sink node for the sensor network charging task and will return to the sink node to receive the charging service when the power is low. The charging efficiency of the MC and the sensor node is η_c. If the power consumed by the MC to charge the sensor node is C, then the power obtained by the sensor node is $\eta_c C$. The lifetime of the MWRSN T_l is the minimum lifetime of a sensor in the set S and can be calculated in the following formula:

$$\begin{aligned} T_l &= \min_{i=1}^{n}(\tau_i) \\ &= \min_{i=1}^{n}\left(\frac{b_i}{e_i}\right). \end{aligned} \tag{1}$$

The lifetime of sensor s_i is τ_i, e_i is the average energy consumption rate of s_i, and n is the number of sensor nodes in the WSN. Considering the actual situation, the charging task interval of MC T_{cti} is defined based on the network lifetime in this paper. If the power of sensor s_i is less than $b_i\omega$, the MC will recharge sensor s_i. Therefore, the charging task interval of MC, T_{cti}, is the time between the completion of charging and the start of the next charging task in this paper. The charging task interval of MC T_{cti} is defined as follows:

$$\begin{aligned} T_{cti} &= \min_{i=1}^{n}\left(\tau_{c,i}\right) \\ &= \min_{i=1}^{n}\left(\frac{b_i(1-\omega)}{e_i}\right). \end{aligned} \tag{2}$$

3.2. WSN Transmission Energy Consumption Model. Here, we consider the radio model and the related parameters referenced in [34]. The energy consumption of each sensor node sends a packet to the next forwarding node over a distance r_c, which is defined as follows:

$$E_T(l, r) = le_{\text{elec}} + l\varepsilon_{fs}r_c^2. \tag{3}$$

The energy consumption of each sensor node receives a packet as shown in the following formula:

$$E_R(l) = le_{\text{elec}}, \tag{4}$$

where l is the packet length, e_{elec} is the energy consumption of the electronic equipment of a bit, and ε_{fs} is the energy consumption of the wireless antenna amplifier. Thus, the energy consumption of i to relay a packet one time is defined as follows:

$$E_i = E_{T,i}(l, r_c) + E_R(l). \tag{5}$$

3.3. WSN Mobile Energy Consumption Model. The mobile energy consumption model of mobile sensor nodes and the MC are referred to in [37]. The wireless sensor network transmission energy consumption model is defined as follows:

$$E_{m,c}\left(d_{m,c}\right) = d_{m,c}e_c, \tag{6}$$

$$E_{m,i}\left(d_{m,i}\right) = d_{m,i}e_{m,i}, \tag{7}$$

where $E_{m,c}(d_{m,c})$ is the mobile energy consumption of the MC and e_c is the energy consumption per unit distance moved by the MC, where $e_c = m_c g\mu_c$, m_c is the mass of the MC, g is the gravitational acceleration, and μ_c is the dynamic friction factor between the MC and the ground. $E_{m,i}(d_{m,i})$ is the mobile energy consumption of sensor s_i, and $e_{m,i}$ is the energy consumption per unit distance moved by sensor s_i, where $e_m = m_{m,i}g\mu_{m,i}$, $m_{m,i}$ is the mass of sensor s_i, and $\mu_{m,i}$ is the dynamic friction factor between sensor s_i and the ground.

3.4. The MWRSN Evaluation Index. The energy consumption of WSN in a charging scheduling cycle contains the energy obtained by the sensors, the moving energy consumption of the MC and sensors, and the energy loss consumed during charging. The payload energy is the energy obtained by the sensors and is defined as E^{pl}. The overhead energy is the moving energy consumption of the MC and sensors during charging and is defined as E^{oh}. The EUE is defined as follows:

$$\text{EUE} = \frac{E^{pl}}{\left(E^{pl} + E^{oh}\right)}. \tag{8}$$

The network lifetime is the time when the first node in the wireless sensor network runs out of energy. The average network lifetime is the average lifetime of MWRSN when the sensor network is randomly deployed for many times in the case of the same battery capacity. The average network energy consumption per unit time is the ratio of wireless transmission energy consumption of MWRSN to the same charging task interval under multiple random deployments of MWRSN. The mobile energy consumption is the moving energy consumption of the MC and mobile sensors. The average mobile energy consumption is the average moving energy consumption of the MC and mobile sensors under multiple random deployments of MWRSN. Charging task scheduling times is the number of charging scheduling performed by MC at the same battery capacity. Average charging scheduling times are the average number of MC

charging task scheduling times when the sensor network is randomly deployed for many times in the case of the same battery capacity.

To better evaluate the mobile sensor network charging model, in addition to energy efficiency, network lifetime, and energy consumption, the average moving loss per unit time (AMUT) is introduced to evaluate the mobile energy cost of the MWRSN charging task. In a charging task interval, the moving energy consumption of a mobile rechargeable sensor network E^{me} mainly includes the moving energy consumption of the MC and sensor nodes. For the whole MWRSN, the moving energy consumption E^{me} is the lower the better. The charging task interval T_{cti} of MWRSN is the longer the better. The AMUT is defined as follows:

$$\mathrm{AMUT} = \frac{E^{\mathrm{me}}}{T_{cti}}. \tag{9}$$

3.5. Main Symbols in Section 3. The main symbols in Section 3 are shown in Table 1.

4. Cooperative Mobile Recharge Method

The cooperative mobile recharge method of MWRSN based on the Hamiltonian path (STCI-TR) in this paper consists of six parts: charging task scheduling request, determining stop position of the MC, determining the charging sensor set, determining stop-wait charging sensor set and stop-wait position, establishing the Hamiltonian path, and cooperative charging. The flowchart of the STCI-TR algorithm is shown in Figure 1.

4.1. Definitions and Assumptions. The definitions used in the cooperative mobile recharge method of MWRSN are as follows:

The *network lifetime* is the time when the first node in the wireless sensor network runs out of energy [22]

The *charging task interval* is the time from the beginning of a charging task to the beginning of the next charging task for the MC in the sensor network

The *stop position* is the best location for the MC as a mobile sink node to collect data in WRSN after the charging scheduling task is completed by the MC

The *stop-wait position* is the location where the MC and the stop-wait charging sensor nodes meet to charge during the process of the MC moving and charging along the specified path

The *energy usage effectiveness* is the ratio of the effective energy obtained by WRSN to the total energy cost of the MC and sensor nodes during the charging process [30]

The assumptions in the wireless rechargeable sensor network model are as follows:

Assumption 1: the sensor node in the mobile rechargeable sensor network sends a 256 bit packet per second for data transmission.

Assumption 2: the sink node and the MC are able to obtain the geographic location (such as through BeiDou, GPS positioning, or other positioning methods) of all nodes in the wireless sensor network.

Assumption 3: the connectivity of the mobile rechargeable sensor network is at least 2 connections. This means that at least 2 nodes are deleted to destroy the connectivity of the network.

Assumption 4: the coverage of the mobile rechargeable sensor network is at least 2 times the coverage. This means that every point in the monitoring area can be covered by at least 2 sensor nodes.

Assumption 5: after the low power prompt of the node in MWRSN, the remaining lifetime of the node can ensure that the MC will arrive at the node. Node failure will not occur due to power exhaustion before charging.

4.2. Charging Task Scheduling Request. When the power of sensor s_i is less than $b_i\omega$, sensor s_i will send the charging request message (*CRequest* (i)) to the MC. After receiving the message *CRequest* (i), the MC will collect the residual power, geographical location, and low-power indicator percentage of all sensors in the MWRSN. In practical application, the power information of the sensor nodes changes little in a short time. To reduce the unnecessary energy, the sensor will carry its own information (including residual power b_i', geographical location $l_{i,}$, and low power indicator percentage ω) when sending data to sink nodes. The maximum lifetime τ_i and residual lifetime τ_i' of sensor s_i will be calculated by the MC according to this information. Next, the MC determines its stopping position according to the collected information.

4.3. Determining the Stop Position of the MC. The stopping position in this paper refers to the optimal position for the MC to collect data as a mobile sink node after the charging scheduling task is completed. To prolong the network lifetime and reduce the overall energy consumption of the network, after the charging is completed, the MC will move to the stop position as mobile sink nodes for the data acquisition task. The MC will wait for the next round of charging task scheduling at the stop position. The new data transmission path of the MWRSN will be planned according to the movement of the MC and its position. The stop position of the MC will affect the lifetime and energy consumption of wireless rechargeable sensor networks. Therefore, it is a key point of this algorithm to determine the appropriate stopping position.

4.3.1. Stop Position Problem of MC. Assume $S = \{s_i: 1, 2, \ldots, n\}$ is the set of WSNs, and the location of mobile wireless sensor node s_i is $l_i = (x_j, y_j)$. The nodes of the wireless rechargeable sensor network are divided into a service group

Table 1: Table of main symbols in Section 3.

Symbol	Parameter
l_i	Location of mobile wireless sensor node s_i
v_i	Average moving velocity of sensor s_i (m/s)
b_i	Battery capacity of s_i (J)
e_i	Average energy consumption rate (J/s)
$e_{m,i}$	Energy consumption of s_i moving one unit distance (J/m)
τ_i	Maximum lifetime of node s_i (s)
$\tau_{c,i}$	Charge cycles of sensor s_i (s)
Ω	Low power indicator percentage of the sensors (%)
B_C	Battery capacity of the MC (KJ)
v_c	Average moving velocity of the MC (m/s)
η_c	Charging efficiency of the MC and the sensor node (%)
T_l	Lifetime of the MWRSN (s)
T_{cti}	Charging task interval of the MC (s)
r_c	Communication radius (m)
L	Packet length (bit)
E_T (l, r)	Energy consumption of each sensor node sends a packet to the next forwarding node over a distance r_c (J)
E_R (l)	Energy consumption of each sensor node receives a packet (J)
E_i	Energy consumption of i to relay a packet one time (J)
D_i	The data size collected by the sensor node per unit time (bit/s)
e_{elec}	Energy consumption of the electronic equipment of l bit (nJ/bit)
ε_{fs}	Energy consumption of the wireless antenna amplifier (pJ/bit)
$E_{m,c}$ $(d_{m,c})$	Mobile energy consumption of the MC (J)
$m_c g$	Force of gravity in the MC (N)
e_c	Energy consumption per unit distance moved by the MC (J/m)
μ_c	Dynamic friction factor between the MC and the ground
$E_{m,i}$ $(d_{m,i})$	Mobile energy consumption of sensor s_i (J)
$e_{m,i}$	Energy consumption per unit distance moved by sensor s_i (J/m)
$m_{m,i} g$	Force of gravity in sensor s_i (N)
$\mu_{m,i}$	Dynamic friction factor between sensor s_i and the ground
E^{pl}	Payload energy (the energy obtained by the sensors) (J)
E^{oh}	Overhead energy (the moving energy consumption of the MC and sensors and the energy consumed loss during charging) (J)
E^{me}	Moving energy consumption of the MWRSN (J)

of sink S_s and a service group of MC S_m. When sensor node $s_{i,s}$ is served by a sink, $s_{i,s} \epsilon S_s = \{s_{i,s}: 1, 2, \ldots, n_s\}$, its data are transferred to a sink node through one or more hops; then, the decision variable X_i is 1; otherwise, it is 0. When sensor node $s_{j,mc}$ is served by the MC, $s_{j,mc} \epsilon S_s = \{s_{j,mc}: 1, 2, \ldots, n_{mc}\}$, its data are transferred to the MC through one or more hops; then, the decision variable X_j is 1; otherwise, it is 0. $D_{i,s}$ and $D_{i,mc}$ are the amount of data sent per unit time by sensor nodes in the service group of the sink and service group of the MC, respectively. $e_{i,s}$ and $e_{j,mc}$ are the unit energy consumption of sensor nodes in the service group of the sink and service group of the MC, respectively. $b_{i,s}'$ and $b_{j,mc}'$ are the actual remaining power of the sensor nodes in the service group of the sink and the service group of the MC, respectively. $d_{i,s}$ is the Euclidean distance from sensor node $s_{i,s}$ to the sink, and $d_{j,mc}$ is the Euclidean distance from sensor node $s_{j,mc}$ to the MC.

To reduce energy consumption and prolong the network lifetime, it is necessary for the MC to select the location that has a long remaining lifetime and the minimum total distance from each node. The objective function of this problem is to minimize the total weighted distance from the sink service group node to the sink (the sum of the ratio of Euclidean distance $d_{i,s}$ to remaining lifetime of sensor $s_{i,s}$) and from the MC service group node to the MC (the sum of the ratio of Euclidean distance $d_{j,mc}$ to remaining lifetime of sensor $s_{j,mc}$). The sink node and the MC can obtain the geographic location (Assumption 2) of sensors in the wireless sensor network and the network uses the GPSR (greedy perimeter stateless routing) protocol. So the sink node and MC can calculate the $d_{i,s}$ and $d_{j,mc}$ easily. $D_{i,s}$ and $D_{i,mc}$ can be obtained by the sink node and the MC when they collect the data. The sink node and the MC know the geographic location of the sensor nodes in the wireless sensor network and use the GPSR protocol. According to the network topology, it is easy for the sink node to evaluate and calculate the amount of data received and forwarded by each sensor node. Therefore, $e_{i,s}$ and $e_{j,mc}$ can be calculated by the sink node according to formulas (3)–(5). The problem model of the MC stop position is as follows:

$$\min \quad \sum_{i=0}^{n_s} \frac{d_{i,s} X_{i,s}}{\tau_{i,s}'} + \sum_{j=0}^{n_{mc}} \frac{d_{j,mc} X_{j,mc}}{\tau_{j,mv}'}, \tag{10}$$

$$\text{s.t.} \quad \sum_{i=1}^{n} X_i = n_s, \tag{11}$$

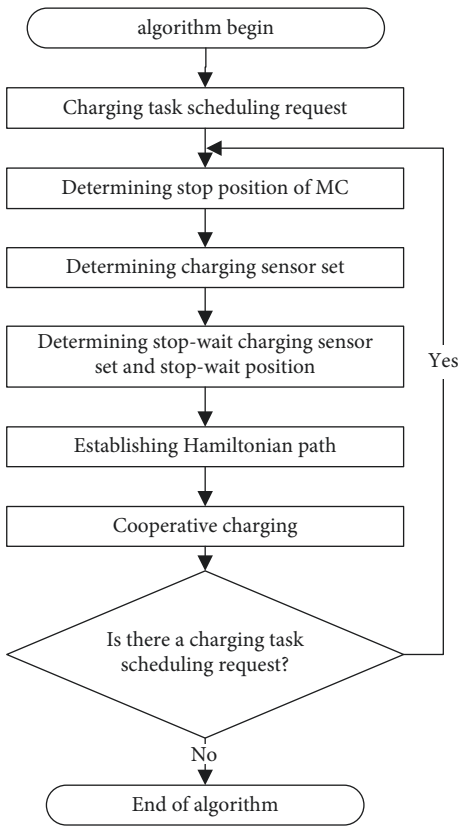

Figure 1: Flowchart of the STCI-TR algorithm.

$$\sum_{j=1}^{n} X_j = n_{mc}, \tag{12}$$

$$n_s + n_{mc} = n, \tag{13}$$

where $\sum_{i=0}^{n_s} d_{i,s}X_{i,s}/\tau_{i,s}'$ is the sum of the ratio of Euclidean distance $d_{i,s}$ to the remaining lifetime $\tau_{i,s}'$ of sensor $s_{i,s}$ and $\tau_{i,s}' = b_{i,s}'/D_{i,s}e_{i,s}$. $\sum_{j=0}^{n_{mc}} d_{j,mc}X_{j,mc}/\tau_{j,mv}'$ is the sum of the ratio of Euclidean distance $d_{j,mc}$ to the remaining lifetime $\tau_{i,mc}'$ of sensor $s_{j,mc}$, and $\tau_{i,mc}' = b_{i,mc}'/D_{i,mc}e_{i,mc}$. The number of sensor nodes in the service group of the sink is n_s and the number of sensor nodes in the service group of the MC is n_{mc}. The number of nodes in the MWRSN is n. The decision variables X_i and X_j are defined as follows:

$$X_i = \begin{cases} 1, & \text{if sensor } s_i \text{ is served by Sink,} \\ 0, & \text{else.} \end{cases}$$
$$X_j = \begin{cases} 1, & \text{if sensor } s_j \text{ is served by MC,} \\ 0, & \text{else.} \end{cases} \tag{14}$$

Constraint formula (11) is the sensor node served by the sink node. Constraint formula (12) is the sensor node served by the MC. Constraint formula (13) ensures that each sensor node can only send data to the nearest sink node or MC, and the sum of the two service group nodes is the number of nodes in the MWRSN.

4.3.2. Solution of Stop Position Problem. To quickly obtain the stopping position of the MC, the Newton method with fast convergence is selected to solve the problem. The specific solution process is as follows:

Step 1: the MC selects the initial point. The MC node starts from the sink node at the beginning, and the coordinate origin (taking the sink node as the coordinate origin) is selected as the initial point. The initial point is defined as $L_{\mathrm{mc},0}(x_0, y_0)$ and $x_0 = y_0 = 0$. The termination error is $\varepsilon > 0$ and let $t = 0$.

Step 2: the MC calculates the gradient vector. Let $f(L_{mc,t}) = \sum_{i=0}^{n_s} d_{i,s}X_{i,s}/\tau_{i,s}' + \sum_{j=0}^{n_{mc}} d_{j,mc}X_{j,mc}/\tau_{j,mv}'$. The gradient vector can be calculated as in formula (15). If the magnitude of the gradient vector is less than the termination error $\|\nabla f(L_{mc,t})\| \le \varepsilon$, the iteration is stopped and the position coordinate $L_{mc,t} = (x_t, y_t)$ is output. Then, the coordinate value is the stop position S_p, and the algorithm ends. Otherwise, go to Step 3.

Step 3: the MC constructs Newtonian directions. MC calculates $[\nabla^2 f(L_{mc,t})]^{-1}$ and constructs Newtonian directions P_t: $P_t = -[\nabla^2 f(L_{mc,t})]^{-1}\nabla f(L_{mc,t})$.

Step 4: find the next iteration point. Let $L_{mc,t+1} = L_{mc,t} + P_t$, $t = t + 1$; return to Step 2.

$$\nabla f(L_{mc,k}) = \begin{bmatrix} \sum_{j}^{n_{mc}} \dfrac{D_{j,mc}e_{j,mc}(x_k - x_{j,mc})X_{j,mc}}{b_{j,mc}'\sqrt{(x_k - x_{j,mc})^2 + (y_k - y_{j,mc})^2}} \\ \sum_{j}^{n_{mc}} \dfrac{D_{j,mc}e_{j,mc}(y_k - y_{j,mc})X_{j,mc}}{b_{j,mc}'\sqrt{(x_k - x_{j,mc})^2 + (y_k - y_{j,mc})^2}} \end{bmatrix}. \tag{15}$$

4.4. Determining the Charging Sensor Set. After the MC stop position is determined, the MC calculates the charging task interval T_{cti} according to its stop position and selects the sensor node. First, the sink node collects information such as the location, residual power, and battery capacity of sensors in the MWRSN. Then, the MC predicts the data transmission path and transmission energy consumption of the sensor nodes according to the information collected by the sink node. The lifetime of the MWRSN T_l and charging task interval T_{cti} can be calculated according to formulas (1) and (2). Finally, according to the calculated charging task interval T_{cti}, the MC selects the sensor node as the element in the charging set S_C of the current scheduling cycle. When $\tau_i' < T_{cti}$, the remaining lifetime of sensor node s_i is less than the charging task interval. Then, the node is added to the charging sensor set $S_c = <s_1, s_2, \ldots, s_q>$.

After determining the charging sensor set S_c, the charging quantity of each charging sensor node in the current round of the charging task should be calculated by the MC. To make the MC charge more sensor nodes, in this model, the MC is not always fully charged when charging the sensor node. The charging task interval is considered, and the charging power of sensor s_i is calculated based on the number of charging task intervals that sensor node s_i

can work at full charge. The charging power of sensor s_i is defined as $b_{i,c}$ and can be calculated in the following formula:

$$b_{i,c} = \left\lfloor \frac{\tau_i}{T_{cti}} \right\rfloor * T_{cti} * e_i - b_i', \tag{16}$$

where b_i' is the remaining battery power of sensor s_i and e_i is the average unit transmission energy consumption of sensor s_i. $\lfloor \tau_i/T_{cti} \rfloor$ is the number of charging task intervals that sensor node s_i can work at full charge.

4.5. Determining Stop-Wait Charging Sensor Set and Stop-Wait Position

4.5.1. Establishing Complete Graph. A complete graph $G(Sink, S_c, S_p)$ is established by the MC. It is composed of the sink node, charging sensor set S_c, and stopping position S_p. In addition, any two points are connected by edges. The MC will construct the Hamiltonian path based on the established complete graph. Initially, the MC starts from the sink node and traverses the charging sensor set $S_c = <s_1, s_2, \ldots, s_q>$ to charge the sensor nodes. After the sensors are charged by the MC, the MC will move to stop position *Sp* as a mobile sink for data collection. The mobile rechargeable sensor network performs routing planning according to the location of sink nodes and the stop position of the MC.

4.5.2. Determining the Stop-Wait Charging Sensor Set. After the charging sensor set S_c is determined, to be able to charge more sensor nodes, the sensor nodes that need to be charged in the next round are also added to this charging task. According to the charging task interval, the MC selects the nodes that need to be charged in the next round as the stop-wait charging sensor nodes. When the survival time of sensor node *si* meets $T_{cti} < \tau_i' < 2T_{cti}$, the *si* node is added to the stop-wait sensor charging set and the stop-wait charging sensor set is determined to be $S_{2,c} = <s_{2,1}, s_{2,2}, \ldots, s_{2,w}>$.

4.5.3. Determining the Stop-Wait Position. In this paper, the stop-wait positions refer to the positions where the MC and stop-wait charging sensor nodes meet to perform cooperative charging during the mobile charging process of the MC in the specified path. When the MC is moving, it will evaluate the time to reach the stop-wait position according to the moving speed of the MC and the distance between the MC and the stop-wait position. Then, the MC will send this information to the stop-wait charging sensor nodes on the path. The stop-wait charging sensor nodes will move according to the received information. Finally, the MC will meet with them at the stop-wait positions to charge the stop-wait charging sensor nodes. To reduce mobile energy consumption, it is important to determine reasonable stop-wait positions. The set of edges in complete graph $G(Sink, S_c, S_p)$ is defined as $E(G) = (E_1, E_2, \ldots, E_{(q+1)\ (q+2)/2})$. Here, q is the number of charging sensor nodes, and the number of edges in complete graph $G(Sink, S_c, S_p)$ is $(q+1)\ (q+2)/2$. The stop-wait position is the position with the shortest distance from the stop-wait sensor node to the edge set $E(G)$ of graph $G(Sink, S_c, S_p)$. The shortest distance $d(s_{2,i})$ from the stop-wait sensor node $s_{2,i}$ to the edge set $E(G)$ can be calculated as in the following formula:

$$d\left(s_{2,i}\right) = \min_{u=1}^{(q+2)(q+1)/2} d\left(s_{2,i}, E_u\right), \tag{17}$$

where E_u is an edge of $E(G)$ and $E_u \epsilon E(G)$. The shortest distance from the stop-wait sensor node $s_{2,i}$ to the edge *Eu* is defined as $d(s_{2,i}, Eu)$. The vector algorithm is used to calculate the shortest distance and determine the stop-wait position. Because of the directionality of the vector, the judgment of the direction can be obtained directly according to its sign, which makes the calculation of the shortest distance and the determination of the stop-wait position easy to solve. Especially when the amount of data to be calculated is large, this method has obvious advantages. $d(s_{2,i}, Eu)$ can be calculated as follows:

$$d\left(s_{2,i}, E_u\right) = \begin{cases} \left|\overrightarrow{s_{u-1}s_{2,i}}\right|, & \text{if } \psi \le 0, \\ \left|\overrightarrow{s_u s_{2,i}}\right|, & \text{if } \psi \ge 1, \\ \left|\overrightarrow{s_{2,pi}s_{2,i}}\right|, & \text{otherwise.} \end{cases} \tag{18}$$

The $d(s_{2,i}, Eu)$ is described in Figure 1. The unit vector in the direction of $\overrightarrow{s_{u-1}s_u}$ is $\overrightarrow{s_{u-1}s_u}/|\overrightarrow{s_{u-1}s_u}|$. $(\overrightarrow{s_{u-1}s_{2,i}}, \overrightarrow{s_{u-1}s_u})$ is the inner product of two vectors, and $(\overrightarrow{s_{u-1}s_{2,i}}, \overrightarrow{s_{u-1}s_u}) = |\overrightarrow{s_{u-1}s_{2,i}}| \cdot |\overrightarrow{s_{u-1}s_u}| \cos\theta$, where θ is the angle between the vectors $\overrightarrow{s_{u-1}s_{2,i}}$ and $\overrightarrow{s_{u-1}s_u}$ and $|\overrightarrow{s_{u-1}s_{2,i}}|$ and $|\overrightarrow{s_{u-1}s_u}|$ are modules of vectors $\overrightarrow{s_{u-1}s_{2,i}}$ and $\overrightarrow{s_{u-1}s_u}$, respectively.

The length of $\overrightarrow{s_{u-1}s_{2,pi}}$ is $(\overrightarrow{s_{u-1}s_{2,i}} \cdot \overrightarrow{s_{u-1}s_u})/|\overrightarrow{s_{u-1}s_u}| = |\overrightarrow{s_{u-1}s_{2,i}}| \cdot |\overrightarrow{s_{u-1}s_u}| \cos\theta/|\overrightarrow{s_{u-1}s_u}|$. The projection vector of $\overrightarrow{s_{u-1}s_{2,i}}$ in the $\overrightarrow{s_{u-1}s_{2,i}}$ direction is $\overrightarrow{s_{u-1}s_{2,pi}}$, and s_2, *pi* is the projection point. The shortest distance is calculated according to the ratio ψ of the projection vector $\overrightarrow{s_{u-1}s_{2,i}}$ to the vector $\overrightarrow{s_{u-1}s_u}$. The ratio ψ can be calculated as $\psi = (\overrightarrow{s_{u-1}s_{2,i}} \cdot \overrightarrow{s_{u-1}s_u})/(\overrightarrow{s_{u-1}s_u} \cdot \overrightarrow{s_{u-1}s_u})$. In Figure 2(a), the stop-wait position of the MC in the edge E_u is $s_{2,pi}$ when $0 < \psi < 1$. In Figure 2(b), the stop-wait position of the MC in the edge E_u is s_u when $\psi \ge 1$. In Figure 2(c), the stop-wait position of the MC in the edge E_u is s_{u-1} when $\psi \le 0$.

4.5.4. Charging Quantity of Stop-Wait Charging Sensors. The mobile energy consumption of the stop-wait charging sensor nodes is considered in the cooperative charging and the charging quantity of the stop-wait charging sensor node $s_{2,i}$ can be calculated by the MC as follows:

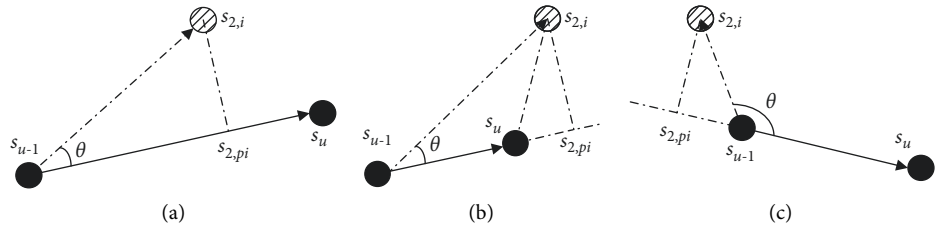

FIGURE 2: The shortest distance from the stop-wait sensor nodes$_{2,i}$ to the edge set E_u: (a) the shortest distance $d(s_{2,i}, E(u))$ when $0 < \psi < 1$; (b) the shortest distance $d(s_{2,i}, E(u))$ when $\psi > 1$; (c) The shortest distance $d(s_{2,i}, E(u))$ when $\psi \le 0$.

$$b_{2,i,c} = \begin{cases} \lfloor \frac{\tau_{2,i}}{T_{ctil}} \rfloor * T_{cti} * e_{2,i} - b_{2,i}' + 2\ d\left(s_{2,i}\right) e_{c,2,i}, \\ \text{if} \quad \lfloor \frac{\tau_{2,i}}{T_{ctil}} \rfloor T_{cti} e_{2,i} + 2\ d\left(s_{2,i}\right) e_{c,2,i} \le b_{2,i}, \\ b_{2,i} - b_{2,i}' + d\left(s_{2,i}\right) e_{c,2,i}, \quad \text{else.} \end{cases} \tag{19}$$

The mobile energy consumption of the stop-wait sensor node $s_{2,i}$ moving from its location to the stop-wait position is $d(s_{2,i})e_{c,2,i}$, where $e_{c,2,i}$ is the energy consumption per unit distance of sensor node $s_{2,i}$. $\lfloor \tau_{2,i}/T_{cti} \rfloor$ is the number of charging task intervals that sensor node $s_{2,i}$ can work at full charge. When the stop-wait charging sensor nodes $s_{2,i}$ and the MC meet at the stop-wait position, the MC will supplement this part of the mobile energy to the stop-wait charging sensor node.

4.5.5. Updating the Stop-Wait Charging Sensor Set. To avoid invalid charging of the stop-wait charge sensor nodes, when the stop-wait charging sensor node occurs as follows, it will be removed from the set of stop-wait charging sensors.

The power of the stop-wait charging sensor node cannot reach the stop-wait position, that is $d(s_{2,i}) e_{c,2,i} > b_{2,i}'$

The moving energy consumption of the stop-wait sensor is greater than its charging capacity, that is, $2 * d(s_{2,i})e_{c,2,i} > b_{2,i,c}$

The lifetime of the stop-wait charging sensor node returning to the original position after charging is less than $2T_{cti}$, that is, $\lfloor \tau_i/T_{cti} \rfloor * T_{cti} * e_{2,i} + 2d(s_{2,i})e_{c,2,i} > b_{2,i}$

If the stop-wait charging sensor node has the above-mentioned situation, the MC will remove it from the set of stop-wait charging sensors and its corresponding stop-wait position.

4.6. Establishing the Hamiltonian Path. The mobile energy consumption of the stop-wait sensor $s_{2,i}$ and the MC are defined as the weight of the edges in the complete graph $G(Sink, S_c, S_p)$. The two charging sensors are defined as s_i, s_j, s_i, $s_j \in S_c$, and $i \ne j$. The weight of edge (s_i, s_j) is defined as $D_h(s_i, s_j) = d(s_i,s_j)e_c + d(s_{2,i})e_{c,2,i}$. Here, $d(s_i,s_j)$ is the Euclidean distance between *si* and *sj*. $d(s_{2,i})$ is the moving distance of the stop-wait charging sensor $s_{2,i}$ from the original position to the stop-wait position. e_c is the mobile energy consumption per unit distance of the MC, and $e_{c,2,i}$ is the mobile energy consumption per unit distance of the stop-wait charging sensor $s_{2,i}$.

According to graph $G(Sink, S_c, S_p)$ and the weights of edges in the graph, the path is selected to minimize the total energy consumption. The essence of this problem is to find a Hamiltonian path with minimum weight in an undirected complete graph with weights, which is a NP complete problem. The proof of a NP complete problem is as follows.

Theorem 1. *The mobile stop-wait charging path problem of MC in MWRSN is a NP complete problem.*

Proof: To prove that the mobile stop-wait charging path problem of MC in MWRSN is NP, we first prove that a special case of the problem is a NP complete problem. The special case of constructing the mobile stop-wait charging path problem is as follows.

The distance $D_h(s_i,s_j)$ between each charging sensor and sink and stop position *Sp* is known. MC should start from the location of the sink node to q charging sensor nodes to charge them, go to stop position *Sp* to collect data as sink node, and return to the starting node after completion.

If charging nodes, sink node, and stop position *Sp* are defined as cities, MC is defined as traveling salesman. The distance $D_h(s_i, s_j)$ between each charging sensor and sink and stop position *Sp* is defined as the distance between cities. Then, the special case is equivalent to the traveling salesman problem (TSP). TSP is a NP complete problem, so this special case is a NP complete problem. Therefore, the mobile stop-wait charging path problem is a NP complete problem.

Due to the imbalance of data transmission tasks in WSN, the number of sensor nodes that need to be charged in each round is smaller than that of the whole network. A simple, practical, and suitable small-scale C-W saving algorithm is selected to solve the Hamiltonian path in this paper. This algorithm was proposed by Clarke and Wright to solve the traveling salesman problem, but it does not consider various constraints. Therefore, it is necessary to consider the energy consumption of the MC and power parameters to improve the C-W algorithm to solve the Hamiltonian path problem of mobile charging.

Let $V(G) = (s_0, s_1, s_2, \ldots, s_q)$ be the set of vertices in graph $G(Sink, S_c, S_p)$, where s_0 is the sink node. The saving value between any two vertices is $CS(s_i, s_j) = D_h(s_0, s_i) + D_h(s_0, s_j) - D_h(s_i, s_j)$, where $s_i, s_j \in S_c$ and $i \ne j$. The larger the $CS(s_i, s_j)$ is,

the greater the reduction in the total cost of connecting s_i and s_j is. When constructing the path, it is sorted in descending order according to the size of $CS(s_i, s_j)$. The specific steps of establishing the Hamiltonian path of MC based on the C-W algorithm are as follows:

Step 1: the saving value $CS(s_i, s_j)$ is calculated and sorted in descending order according to the size of $CS(s_i, s_j)$.

Step 2: determine whether sensor nodes s_i *and* s_j corresponding to the maximum edge of $CS(s_i, s_j)$ in the sequence satisfy the following conditions.

If sensor nodes s_i and s_j are not on the established path, then s_i and s_j can be connected. After connecting, the path is $<s_0 \longrightarrow s_i \longrightarrow s_j \longrightarrow s_0>$ and turns to Step 3.

If sensor nodes s_i and s_j are on the established path but not the inner point in the line (which means that the node is not directly connected to source point s_0), then connect them and turn to Step 3.

If the sensor nodes s_i and s_j are on the established path and all not inner points on the line, then connect them and turn to Step 3.

If the sensor nodes s_i and s_j are on the established path but not the inner point on the line, then do not connect them and turn to Step 4.

Step 3: The sum mobile energy consumption to traverse the connected path is calculated by MC $\mathrm{Sum}(E^{oh}_{G,c,m})$, and the sum energy of the sensor nodes needs to be charged in the path $\mathrm{Sum}(b_{G,c})$. If $\mathrm{Sum}(E^{oh}_{G,c,m}) + \mathrm{Sum}(b_{G,c}) > P'$ (which means that the remaining power of MC P' is insufficient to complete the charging of this path), the MC removes the path from sensor node s_i to other nodes. Then, turn to Step 5; otherwise, turn to Step 4.

Step 4: The MC removes the path from sensor node s_i to other nodes. When all the paths of charging sensors are removed, the complete Hamiltonian path is obtained and the algorithm terminates. Otherwise, the MC selects the node with the maximum saving value from the path of sensor nodes not removed and turns to Step 2.

Step 5: When the remaining power of the MC is enough to reach the sink node, the MC connects the sink node to the next path node of sensor node s_i. When the remaining power of the MC cannot reach the sink node, the MC removes sensor node s_i and the previous path node of sensor node s_i is selected to connect with the sink node. Then, the MC replenishes the power at the sink node, and after electricity replenishment is completed, the MC establishes the complete graph composed of the sink node, the stop position, and the remaining unconnected nodes. Return to Step 1 and reestablish the Hamiltonian path. □

4.7. Cooperative Charging. According to the established Hamiltonian path, the MC moves along edges $E_1 = <s_0, s_1>$, $E_2 = <s_1, s_2>$, . . ., $E_q = <s_{q-1}, s_q>$, $E_{q+1} = <s_q, s_0>$. In the beginning, the MC starts from the sink (s_0) node, and when there is a stop-wait position at edge E_1, the MC stops at this position and meets with stop-wait charging sensor nodes $s_{2,1}$ to charge. After charging the stop-wait charging sensor nodes $s_{2,c}$, the MC moves to the position of charging sensor node s_1 and charges s_1. The MC will traverse the edges $E(G) = (E_1, E_2, \ldots, E_{q+1})$ and charge the sensor node.

To save charging scheduling time, according to the position and moving speed of the MC, the time to reach the stop-wait position is calculated by the stop-wait charging sensor $s_{2,i}$ of $S_{2,c}$. The stop-wait charging sensor $s_{2,i}$ adjusted its moving speed to ensure that it reached the stop-wait position at the same time as the MC. Then, the stop-wait sensor nodes meet with the MC at the stop-wait position to charge the sensor nodes. This method can save the mobile energy consumption of the MC and improve the charging efficiency. Finally, after the MC charges the stop-wait sensor nodes in the path, the stop-wait charging sensor nodes will return to their original positions. The MC continues to traverse the path of the Hamiltonian loop and charge the sensor nodes.

The MC and stop charging sensor nodes will send their location information to their neighbor sensor nodes during the mobile charging process. When the neighboring sensor nodes receive the location information, they will share it with other sensor nodes. The sensor nodes in the network reconstruct the network topology according to the location of the MC, stop-wait charging sensor nodes, and sink nodes. When the MC completes the charging task, they will return to the stop position and wait for the next round of charging task scheduling. At this point, the MC will perform collaborative data collection as a sink node, and the collected data will be transmitted by 4G or 5G technology to the sink node or Data center. The MC will also send its location information to its neighboring sensor nodes. The sensor nodes in the network replan their routing paths according to the location of the sink node and the MC to reduce the excessively long path from some nodes to sink nodes, thus reducing network energy consumption.

4.8. Algorithm Description and Analysis. The description of the MWRSN charging task coordination algorithm based on the Hamiltonian path is shown in Algorithm 1.

Table 2 shows a comparison of the time complexity using the DPMCS [21], MUC [34], BNRS [35], VN-MOAC [36], and STCI-TR algorithms. The n_t is defined as the number of time steps in each episode and n_m is the number of episodes.

The time complexity of the STCI-TR algorithm is $O(n^2)$. The number of charging sensors q and the stop-wait charging sensor w are the problem size. The time complexity of the shortest distance $d(s_{2,i})$ with the number of sensors q is $T(q) = (q + 2)\ (q + 1)/2$. The time complexity to compute the saving value $C_S(s_i, s_j)$ with the number of sensors q and the stop-wait charging sensor w is $T(q + w) = 3(q + w + 1)^2$. So the time complexity of the algorithm is $O(n^2)$.

The algorithm example is shown in Figure 3. In the power grid substation field, the substation inspection robots are used for condition monitoring of electrical equipment. The mobile vehicle can be integrated with data collection

(1) The sensor node s_i initializes the ID_i, l_i and v_i
(2) Initial network topology of the MWRSN
(3) **while** ($\exists b_i'/b_i < \omega$) **do**
(4) The sensor node s_i send charging request message (*CRequest*)
(5) MC calculates T_{cti} and T_l according to b_i', l_i, ω after receiving *CRequest*
(6) MC calculates its stop position (x_{sp0}, y_{sp0})
(7) MC calculates T_{cti} and T_l according to its stop position
(8) **for (i = 1, i++, i ≤ n) do**
(9) **if** ($\tau_i' < T_l$) **do**
(10) The s_i is added to set $S_c = <s_1, s_2, \ldots, s_q>$ by MC, where $q \leq n$
(11) MC calculates the charging power of the sensors in set S_c
(12) **end if**
(13) **if** ($T_l < \tau_i' < 2 * T_l$) **do**
(14) MC establishes the $G(S_p, S_c, Sink)$ and determines the set $S_{2,c}$
(15) MC determines stop-wait position, and charging power of $S_{2,c}$
(16) **end if**
(17) **end for**
(18) MC establishes the Hamiltonian path according to section E of the part III
(19) MC moves along edge $E_1 = <s_0, s_1>$, $E_2 = <s_1, s_2>$, $\ldots$, $E_q = <s_{q-1}, s_q>$, $E_{q+1} = <s_q, s_0>$
(20) **if** (There are stop-wait positions in edge E_1)**then**
(21) Stop-wait sensor $s_{2,i}$ meets with MC for cooperative charging
(22) After the $s_{2,i}$ is charged, it will return to its original positions
(23) **end if**
(24) After MC completes charging task, it will return to stop position
(25) **end while**

Algorithm 1: The MWRSN charging task cooperative algorithm based on the Hamiltonian path (STCI-TR).

Table 2: Simulation parameters.

Algorithm	Maximum problem size	Time complexity
MUC	$6.5n^2 + 23.5n + 9$	$O(n^2)$
BNRS	$5n^2 + 12n + 3$	$O(n^2)$
DPMCS	$8n_t * n_m + 2n_m + 2$	$O(n^2)$
VN-MOAC	$n + n^2 * \lg n^2$	$O(n^2 \lg n^2)$
STCI-TR	$3.5n^2 + 13.5n + 5$	$O(n^2)$

equipment and the energy transmitter as MC to charge these substation inspection robots. The sink node is used for data aggregation and transfer the data to the substation monitoring center. MC also can replenish the power at the sink node.

We assumed that there are 12 substation inspection robots as mobile rechargeable sensor nodes (s_1, s_2, $\ldots$, s_{12}) deployed in a two-dimensional scene, and the MC starts from the position of the sink node and charges the sensor node. At the beginning of the algorithm, we assumed that the power of sensor node s_1 is lower than the low power indicator percentage ω, and the charging task request information *CRequest* is sent to the MC. After the MC receives the charging task request, the MC collects the remaining power b_i', position information $l_{i,}$, and the percentage of power. Then, MC calculates the charging cycle τ_i and the actual lifetime τ_i' of the sensor node.

The MC determines its stop position ${}^{(1)}S_p$ in the first round. The MC determines the charging sensor set and selects the charging sensor set ${}^{(1)}S_c = (s_1, s_2, s_3, s_4, s_5)$ in this example. The MC determines the stop-wait charging sensor set and corresponding stop-wait position. The selected stop-wait set is ${}^{(1)}S_{2,c} = (s_6, s_7, s_8)$ and corresponding stop-wait positions are $s_{2,p6}$, $s_{2,p7}$, $s_{2,p8}$. The Hamiltonian path $<Sink \longrightarrow s_1 \longrightarrow s_2 \longrightarrow s_3 \longrightarrow s_4 \longrightarrow s_5 \longrightarrow {}^{(1)}S_p \longrightarrow Sink>$ is established.

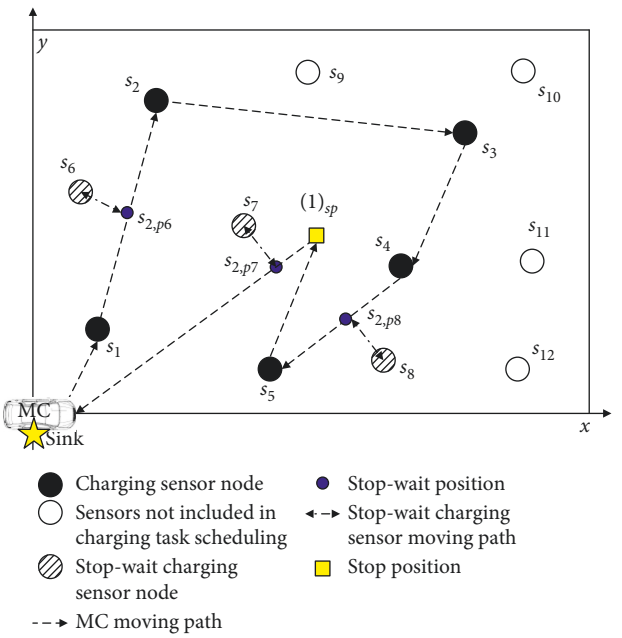

Figure 3: Schematic diagram of the STCI-TR algorithm example.

The MC moves to charge the sensor nodes. The MC moves along edges $E_1 = <s_0, s_1>$, $E_2 = <s_1, s_2>$, $E_3 = <s_2, s_3>$, $E_4 = <s_3, s_4>$, $E_5 = <s_4, s_5>$, $E_6 = <s_5, {}^{(1)}S_p>$, and $E_7 = <{}^{(1)}S_p,$

Table 3: Table of main symbols in Section 4.

Symbol	Parameter
S_s	Service group of the sink
S_m	Service group of the MC
$s_{i,s}$	Sensor node is served by the sink node
$s_{j,mc}$	Sensor node is served by the MC
X_j	Decision variable (0 or 1)
$D_{i,s}$	Amount of data sent per unit time by $s_{i,s}$ in the S_s (bit/s)
$D_{i,mc}$	Amount of data sent per unit time by $s_{j,mc}$ in the S_m (bit/s)
$e_{i,s}$	The unit energy consumption of sensors in the S_s (J/s)
$e_{j,mc}$	The unit energy consumption of sensors in the S_s(J/s)
$b_{i,s}{}'$	The actual remaining power of sensor nodes in the S_s(J)
$b_{j,mc}{}'$	The actual remaining power of sensor nodes in the S_m (J)
$d_{i,s}$	Euclidean distance from sensor node $s_{i,s}$ to the sink (m)
$d_{j,mc}$	Euclidean distance from sensor node $s_{j,mc}$ to the MC (m)
$\tau_{i,s}{}'$	Remaining lifetime of sensor $s_{i,s}$ (s)
$\tau_{i,mc}{}'$	Remaining lifetime of sensor $s_{j,mc}$ (s)
n_s	The number of sensor nodes in the S_s
n_{mc}	The number of sensor nodes in the S_m
$L_{mc,0}$	The initial point of the MC (0, 0)
$L_{mc,t}$	The location of the MC after iterative t-round
S_p	The MC stop position
S_c	The charging set
$b_{i,c}$	The charging power of sensor s_i
G	Complete graph G *(Sink,* S_c, S_p*)* established by MC
$S_{2,c}$	The stop-wait sensor charging set, ($s_{2,i} \epsilon S_{2,c}$)
$E(G)$	The set of edges in complete graph G *(Sink,* S_c, S_p*)*
Q	The number of charging sensor nodes
$d(s_{2,i})$	The shortest distance from the $s_{2,i}$ to the edge set $E(G)$
$d(s_{2,i}, Eu)$	The shortest distance from the $s_{2,i}$ to the edge E_u
Θ	The angle between the vectors $\overrightarrow{s_{u-1}s_{2,i}}$ and $\overrightarrow{s_{u-1}s_u}$
Ψ	The ratio of the projection vector $\overrightarrow{s_{u-1}s_{2,i}}$ to $\overrightarrow{s_{u-1}s_u}$
$b_{2,i,c}$	The charging quantity of the stop-wait charging sensor node $s_{2,i}$
$e_{c,2,i}$	The energy consumption per unit distance of sensor node $s_{2,i}$
$D_h(s_i, s_j)$	The weight of edge (s_i, s_j)
$V(G)$	The set of vertices in graph G*(Sink,* S_c, S_p*)*
$C_S(s_i, s_j)$	The saving value between vertices s_i and s_j
$\mathrm{Sum}(E^{oh}_{G,c,m})$	The sum mobile energy consumption to traverse the connected path
$\mathrm{Sum}(b_{G,c})$	The sum energy of the sensors needs to be charged in path
P'	The remaining power of MC

s_0>. In the initial stage, the MC starts from sink node (s_0) to s_1, and there is no stop-wait position in E_1. The MC moves directly to s_2, and there is stop-wait position $s_{2,p6}$ in E_2. Then, the MC moves to $s_{2,p6}$ and meets this position with sensor $S_{2,1}$ to charge. When sensor $S_{2,1}$ is charged by the MC, the MC will continue to move until the charging of sensor nodes in S_c and $S_{2,c}$ is completed. Finally, the MC moves along $E_6 = <s_5, {}^{(1)}S_p>$ to stop position ${}^{(1)}S_p$ for data collection.

4.9. Main Symbols in Section 4. The main symbols in Section 4 are shown in Table 3.

5. Simulation Results and Analysis

In this section, the proposed algorithms are validated by comparing their performances with other mobile recharge schemes in terms of the EUE, network lifetime, and average moving loss per unit time. There is a sink node to collect the information and an MC to charge the sensors in the MWRSN. Simulink in MATLAB 2012 is used to test the algorithm performances. The performance of DPMCS [21], MUC [34], BNRS [35], VN-MOAC [36], and STCI-TR algorithms are compared by simulation. The DPMCS considers the dynamic topology of WSN and uses deep reinforcement learning to determine the schedule of the mobile charger. In BNRS, the moving path of MCs along power banks is optimized so that every power bank can be recharged before falling below a critical threshold. To improve the operation time of the nodes, the energy quota of each node is calculated based on its energy consumption level. The directed coverage subsets with the largest charging gain in WSN are first searched in MUC. Then, the charging anchor points are determined according to the directed coverage subset and the charger movement path is planned. Finally, the constraints of mobile charger energy and charging cycle are considered and the charging time is optimized. In VN-MOAC, charging requirements and data

Table 4: Simulation parameters.

Symbol	Parameter	Value
$r_{t,i}$	Transmission rate of sensor s_i	128 kbps
$r_{c,i}$	Communication radius of sensor s_i	50 m
lp	Packet length of the sensor	256 bit
e_{elec}	Energy consumption of the electronic equipment of l bit	50 nJ/bit
ε_{fs}	Energy consumption of the wireless antenna amplifier	10 pJ/bit
m_c	The mass of MC	1.5 kg
g	Gravitational acceleration	9.8 m/s^2
μ_c	Dynamic friction factor between the MC and the ground	0.7
e_c	Energy consumption per unit distance moved by the MC	6.91 J/m
$m_{m,i}$	The mass of sensor s_i	0.2 kg
$\mu_{m,i}$	Dynamic friction factor between the MC and the ground	0.47
$e_{m,i}$	Energy consumption per unit distance moved by sensor s_i	0.92 J/m
B_{C}	Battery capacity of the MC (kJ)	80 kJ
b_i	Initial power of all of the sensors	1000 J

collecting are taken into consideration simultaneously. A one-to-many charging and data collecting model for MC is established with two optimization objectives, maximizing the total energy utilization and minimizing the average delay of data collecting.

5.1. Simulation Parameters. In the communication simulation, the transmission rate of the ZigBee 802.15.4 protocol is selected in our simulation model. The detailed simulation parameters are shown in Table 4.

The maximum data transmission rate of this protocol is 250 kbps. The median value (128 kbps) is selected as the simulation parameter. The packet length of ZigBee 802.15.4 protocol ranges from 128 bit to 127 byte. The packet length of the sensor in the simulation is $l_p = 256$ bit. Literature [38] proposed an algorithm to generate the unified dataset for the general and some specific applications system models in WSNs. The results produced by the proposed algorithm reflect the pseudorandomness. Therefore, the standard datasets in [38] are used to evaluate our methods and the comparison algorithms. The routing protocol is greedy perimeter stateless routing (GPSR). Fifty sensor nodes are randomly deployed in a 400×400 m area. These nodes are subject to a uniform random distribution; that is, the horizontal and vertical coordinates of 50 sensor nodes corresponding to two groups of uniformly distributed random numbers (50 for each group) are generated in 0–400 m, and then, the deployment position is determined. The moving speed of the sensors and MC is 2 m/s according to [34]. We consider the communication energy parameters referenced in [39]. The communication energy parameters are set as $e_{elec} = 50\ \mu$J/bit and $\varepsilon_{fs} = 10$ nJ/bit. The communication radius is $r_{c,i} = 50$ m. The initial energy of the sensor is set $b_i = 1000$ J, and the battery capacity of the MC is set $B_C = 80$ KJ according to [36]. The mass of MC is set $m_c = 1.5$ kg, and the mass of sensor s_i is set $m_{m,i} = 0.2$ kg. The dynamic friction factor is set $\mu_c = \mu_{m,i} = 0.47$ according to [40]. The moving energy consumption of the sensor node $e_s = 0.92$ J/m can be calculated according to formula (6). The moving energy consumption of the MC $e_c = 6.91$ J/m can be calculated according to formula (7).

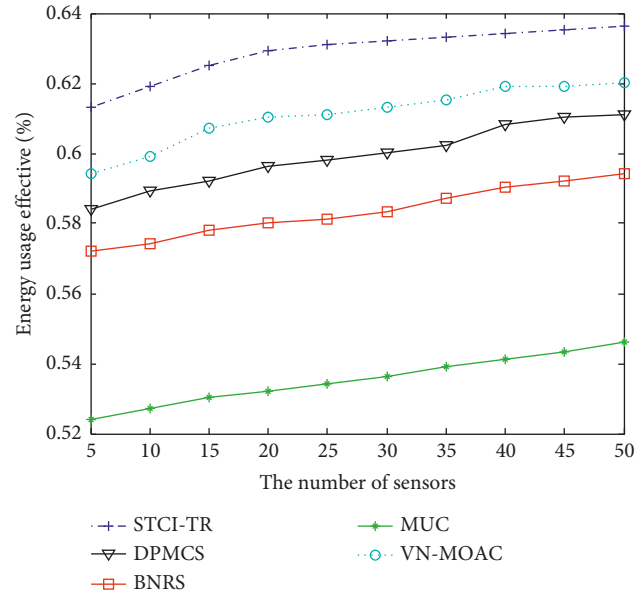

Figure 4: Comparison of the EUE with different numbers of sensor nodes.

5.2. EUE Analysis of the Algorithm. Figure 4 shows a comparison of the EUE with different numbers of sensors using the DPMCS, MUC, BNRS [35], VN-MOAC, and STCI-TR algorithms.

In Figure 4, the EUE of nodes decreases little with the increase in the number of nodes. This is because the energy consumption increase caused by the movement of the MC during charging accounts for a small proportion of the total energy consumption. The STCI-TR algorithm takes the MC as a sink node for collaborative collection, which improves the network lifetime. Therefore, the EUE of STCI-TR is 17.56% higher than that of MUC and 8.07% higher than that of BNRS. The charging sensor node of the next round is considered in the STCI-TR algorithm for the current charging task scheduling. It avoids the MC charging the node in the next round and reduces the mobile energy consumption of MC. So the EUE of STCI-TR is 4.84% higher than that of DPMCS and 2.94% higher than that of VN-MOAC.

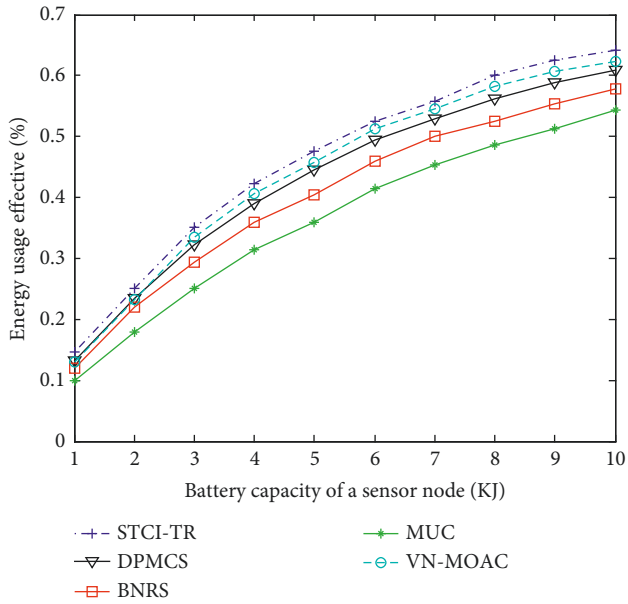

Figure 5: Comparison of the EUE with different node battery capacities.

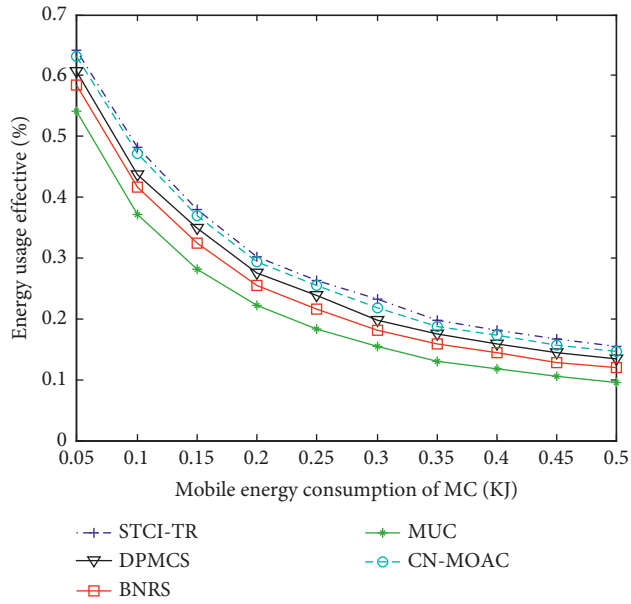

Figure 6: Comparison of EUE with different mobile energy consumptions of MC.

Figure 5 shows a comparison of the EUE with different battery capacities of sensors using the MUC, *BNRS*, DPMCS, VN-MOAC, and STCI-TR algorithms. The EUEs of the nodes are all improved with different battery capacities of the sensor. With the increase in the battery capacity of sensor nodes, the energy of the MC primary charge scheduling is increased. However, the energy consumption caused by the movement does not increase at this time. So the EUEs are improved. The STCI-TR algorithm takes the MC as a sink node for collaborative collection and considers the charging sensor node of the next round for the current charging task scheduling. It reduces the network transmission energy consumption and mobile energy consumption of MC. Therefore, the EUE of STCI-TR is 28.54% higher than that of MCU and 14.87% higher than that of BNRS. The scheduling times of the MC are reduced, and the mobile energy consumption is reduced at the same time. So the EUE of STCI-TR is 6.33% higher than that of DPMCS and 4.84% higher than that of VN-MOAC.

Figure 6 shows the comparison of the EUE with different mobile energy consumption of the MC using the MUC, BNRS, DPMCS, VN-MOAC, and STCI-TR algorithms. The EUEs of all methods decrease with increasing MC mobile energy consumption. This is because the energy consumption increase caused by the movement of the MC during charging accounts for a large proportion of the total energy consumption. So the EUEs are decreased. The STCI-TR algorithm takes the MC as a sink node for a collaborative collection. It reduces the network transmission energy consumption. Therefore, the EUE of STCI-TR is 38.76% higher than that of MUC and 18.64% higher than that of BNRS. The STCI-TR algorithm considers the charging sensor node of the next round for the current charging task scheduling. This method can reduce the mobile energy consumption of MC and the MC scheduling times at the same time. So the EUE of STCI-TR is 9.83% higher than that of DPMCS and 7.05% higher than that of VN-MOAC.

Figure 7 shows the comparison of EUE with different charging efficiencies using the MUC, BNRS, DPMCS, VN-MOAC, and STCI-TR algorithms.

In Figure 7, the EUE of nodes is improved with increasing charging efficiency. This is because the charging energy consumption of the MC during charging is reduced with increasing charging efficiency. However, the network transmission energy consumption and the energy consumption caused by the movement do not increase at this time. So the EUEs are improved. The STCI-TR algorithm takes the MC as a sink node for a collaborative collection. It reduces the network transmission energy consumption. Therefore, the EUE of STCI-TR is 19.56% higher than that of MUC and 14.62% higher than that of BNRS. The STCI-TR algorithm considers the charging sensor node of the next round for the current charging task scheduling. This method can reduce the mobile energy consumption of MC and the MC scheduling times at the same time. Therefore, the EUE of STCI-TR is 5.04% higher than that of DPMCS and 2.78% higher than that of VN-MOAC.

5.3. Network Lifetime Analysis of the Algorithm. Figure 8 shows the comparison of network lifetimes with different numbers of sensor nodes using the MUC, BNRS, DPMCS, VN-MOAC, and STCI-TR algorithms. According to the simulation parameter settings in Table 4 and the transmission energy consumption model of the wireless sensor network in Section 3.3, the lifetime of a single sensor node without moving and one-hop data transmission is approximately 3.125×10^7 s. In Figure 8, the network lifetimes

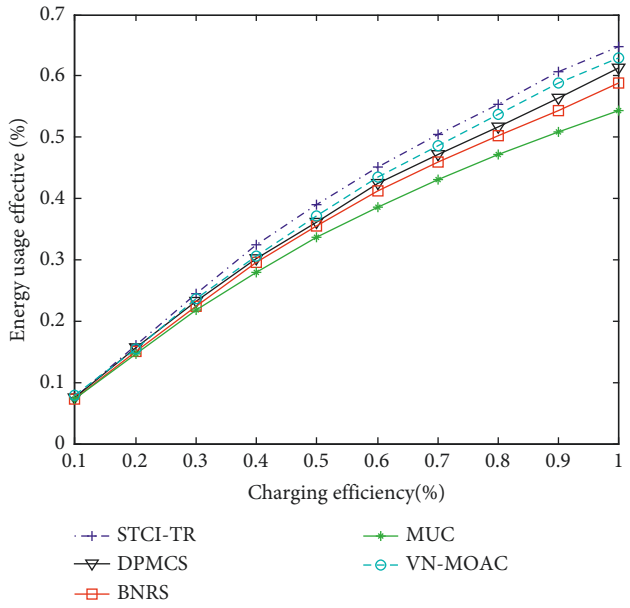

Figure 7: Comparison of the EUE with different charging efficiencies.

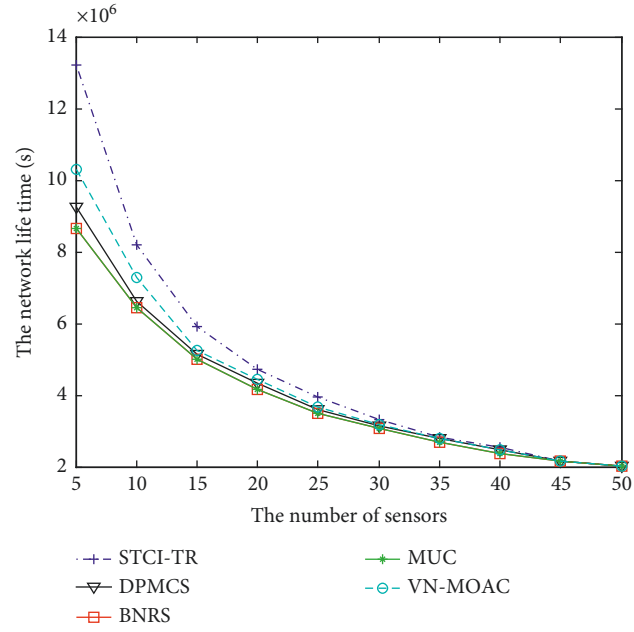

Figure 8: Comparison of network lifetime with different numbers of nodes.

of all methods decrease as the number of sensor nodes increases. This is because the energy consumption of the sensor nodes closest to the sink is increasing and reduces the network lifetime. The STCI-TR algorithm takes the MC as a sink node for a collaborative collection. It reduces the network transmission energy consumption. The STCI-TR can improve the network lifetime and charging task interval. The MC is not considered a sink node for collaborative collection in MCU and BNRS. So they have the same network lifetime. The network lifetime of STCI-TR is 13.08% higher than that of BNRS and MCU. The DPMCS algorithm considers the MC as a sink node to collect the data in the charging process. However, the charging process is shorter than the whole network lifetime and less improved than VN-MOAC and DPMCS. Therefore, the network lifetime of STCI-TR is 10.28% higher than that of DPMCS and 7.04% higher than that of VN-MOAC.

5.4. Average Network Energy Consumption per Unit Time. Figure 9 shows a comparison of the average network energy consumption per unit time with different numbers of sensor nodes using the MUC, BNRS, DPMCS, VN-MOAC, and STCI-TR algorithms. The average network energy consumption per unit time of all methods is improved as the number of sensor nodes increases. This is because the path from some sensor nodes to sink is increasing, and it increases the average network energy consumption per unit time. The STCI-TR algorithm takes the MC as a sink node for a collaborative collection. After the charging and the completion of charging, the route planning is carried out again. It reduces the path length from some sensor nodes to sink and MC and the network transmission energy consumption. The MC is not considered a sink node for collaborative collection in BNRS and MCU, so they have the same average network energy consumption per unit time. The average network energy consumption per unit time of STCI-TR is 6.73% lower than that of BNRS and MCU. The DPMCS and VN-MOAC algorithms consider MC as a sink node to collect the data in the charging process. However, the MC is not used as a sink node for collaborative collection in DPMCS and VN-MOAC after charging scheduling. The STCI-TR algorithm reduces the length of the route path from some sensor nodes to sink and MC before the next round of charging task scheduling requests. So the reduced network energy consumption of DPMCS and VN-MOAC is less than that of STCI-TR. Therefore, the average network energy consumption per unit time of STCI-TR is 2.68% lower than that of VN-MOAC and 4.76% lower than that of DPMCS.

5.5. Average Movement Loss per Unit Time. Figure 10 shows a comparison of the average moving loss per unit time with different numbers of sensor nodes using MUC, BNRS, DPMCS, VN-MOAC, and STCI-TR algorithms. The average moving loss per unit time of all methods increases as the number of sensor nodes increases. This is because the mobile energy consumption caused by the MC charging is increasing, and the average mobile loss per unit time is also increasing. The STCI-TR algorithm takes the MC as a sink node for collaborative collection, which improves the network lifetime and reduces the MC scheduling times and average moving loss per unit time at the same time. The MC is not considered a sink node for collaborative collection in MUC and BNRS. This causes the transmission path of some sensor nodes to be too long and increases the network transmission energy consumption. It increases the MC scheduling frequency and average moving loss per unit time.

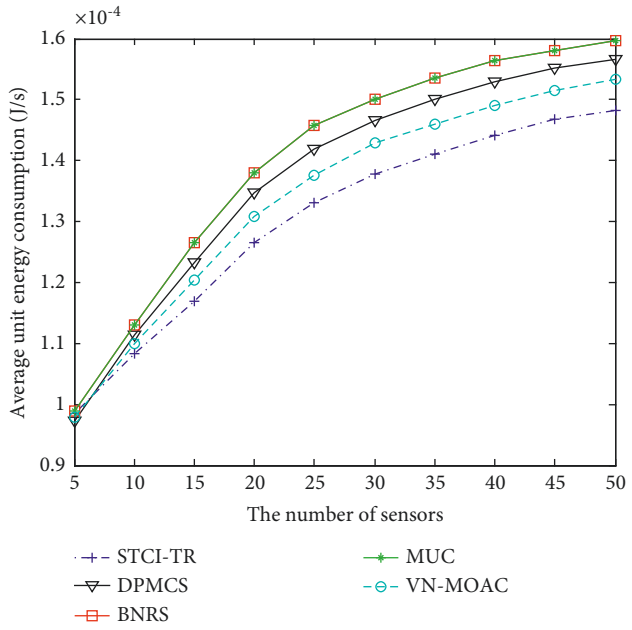

Figure 9: Comparison of average network energy consumption with different numbers of nodes.

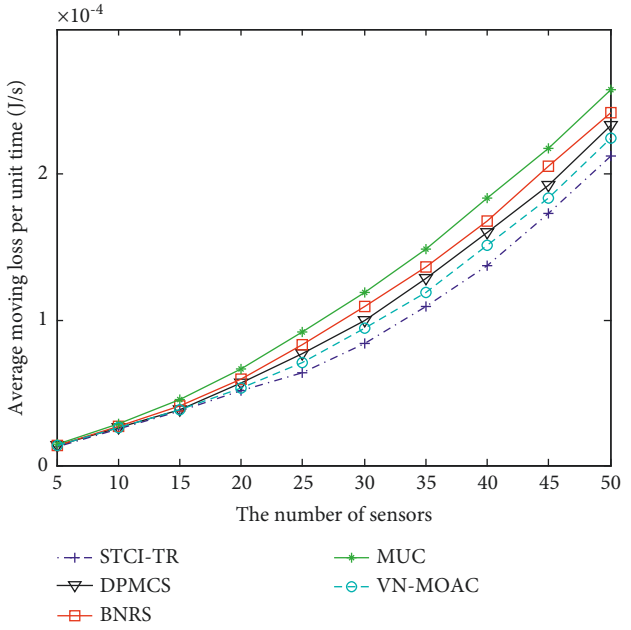

Figure 10: Comparison of average moving loss per unit time with different numbers of nodes.

The average moving loss per unit time of STCI-TR is 26.74% lower than that of MCU and 16.96% lower than that of BNRS. The DPMCS and VN-MOAC algorithms consider MC as a sink node to collect the data in the charging process. However, the charging process is shorter than the whole network lifetime. The network transmission energy consumption of DPMCS and VN-MOAC is less reduced than STCI-TR. The STCI-TR algorithm also considers the charging sensor node of the next round for the current charging task scheduling. It can also reduce the mobile energy consumption of MC and the MC scheduling times at the same time. Therefore, the average moving loss per unit time of STCI-TR is 9.95% lower than that of DPMCS and 6.87% lower than that of VN-MOAC.

5.6. Average Mobile Energy Consumption. Figure 11 shows a comparison of the average mobile energy consumption with different numbers of sensor nodes using MUC, BNRS, DPMCS, VN-MOAC, and STCI-TR algorithms.

The average mobile energy consumption of all methods increases as the number of sensor nodes increases. As the number of nodes increases, the number of nodes that need to be charged by MC for each charging schedule also increases. So the moving distance of MC becomes longer and mobile energy consumption caused by the MC is increasing. The STCI-TR algorithm considers the charging sensor node of the next round (the stop-wait sensor nodes) for the current charging task scheduling. In the next round, the number of nodes that need to be charged by MC will be reduced. Therefore, the average mobile energy consumption of STCI-TR is lower than that of MCU, BNRS, DPMCS, and VN-MOAC.

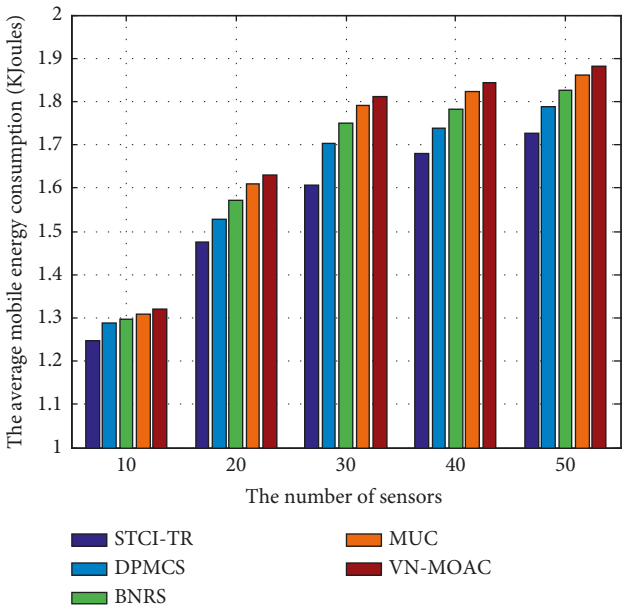

Figure 11: Comparison of average mobile energy consumption with different numbers of nodes.

5.7. Average Charging Task Scheduling Times. Figure 12 shows a comparison of the average charging task scheduling times with different numbers of sensor nodes using MUC, BNRS, DPMCS, VN-MOAC, and STCI-TR algorithms. According to the simulation parameter settings in Table 3, the charging task interval of these algorithms is 2.0×10^6 s (it is the average value of the simulation with 50 sensor nodes). The average charging task scheduling times of all methods decrease as the number of sensor nodes

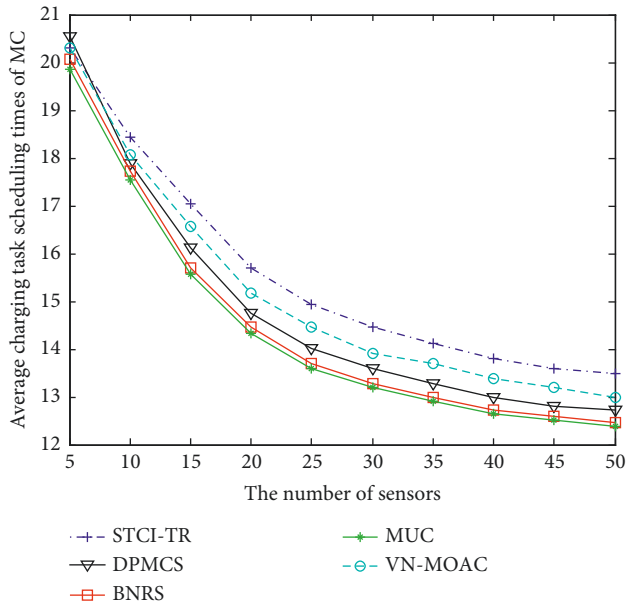

Figure 12: Comparison of average charging task scheduling times with different numbers of nodes.

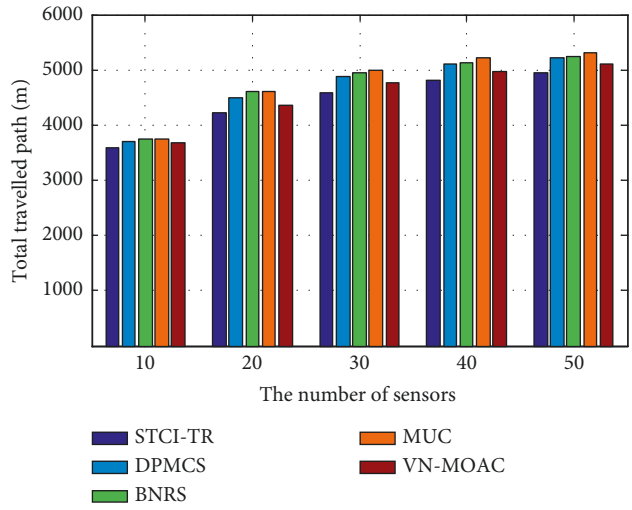

Figure 13: Comparison of the total travelled path with different numbers of nodes.

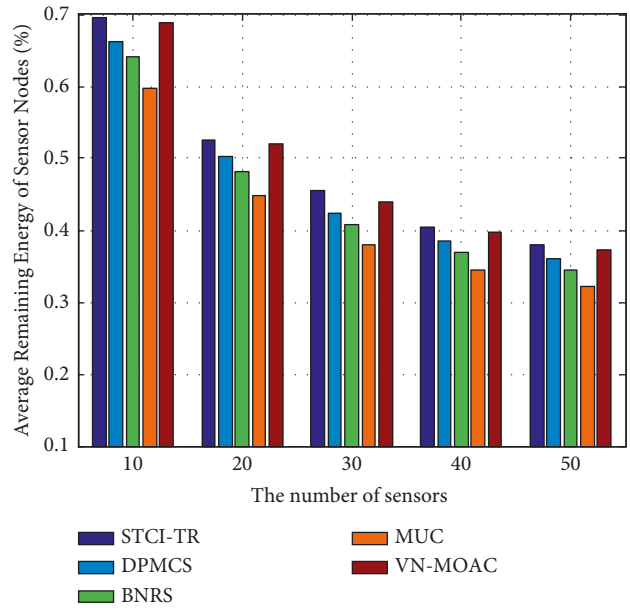

Figure 14: Comparison of average remaining energy with different numbers of nodes.

increases. As the number of nodes increases, the mobile energy consumption caused by the MC moving is increasing and the average network energy consumption is also increasing. The STCI-TR algorithm takes the MC as a sink node for a collaborative collection. It reduces the network transmission energy consumption. The MC is not considered a sink node for collaborative collection in MCU and BNRS. So the average charging task scheduling times of STCI-TR is 7.52% higher than that of MCU and 6.81% higher than that of BNRS.

The DPMCS and VN-MOAC algorithms consider MC as a sink node to collect the data in the charging process. However, the charging process is shorter than the whole network lifetime. The network transmission energy consumption of DPMCS and VN-MOAC is less reduced than STCI-TR. The STCI-TR algorithm considers the charging sensor node of the next round (the stop-wait sensor nodes) for the current charging task scheduling. In the next round, the number of nodes that need to be charged by MC will be reduced and can also reduce the mobile energy consumption of MC. Therefore, the average charging task scheduling times of STCI-TR is 4.73% higher than that of DPMCS and 2.52% higher than that of VN-MOAC.

5.8. Total Travelled Path. Figure 13 shows a comparison of the total travelled path with different numbers of sensor nodes using MUC, BNRS, DPMCS, VN-MOAC, and STCI-TR algorithms. The total travelled path of all methods increases as the number of sensor nodes increases. As the number of nodes increases, the number of nodes that need to be charged by MC for each charging schedule also increases. So the moving distance of MC becomes longer and the total travelled path caused by the MC is increasing. The STCI-TR algorithm considers the charging sensor node of the next round (the stop-wait sensor nodes) for the current charging task scheduling. In the next round, the number of nodes that need to be charged by MC will be reduced. Therefore, the total travelled path of STCI-TR is lower than that of MCU, BNRS, DPMCS, and VN-MOAC.

5.9. Average Remaining Energy. Figure 14 shows a comparison of the average remaining energy with different numbers of sensor nodes using MUC, BNRS, DPMCS, VN-MOAC, and STCI-TR algorithms. The average remaining energy of all methods decreases as the number of sensor nodes increases. As the number of nodes increases, the

number of nodes that need to be charged by MC for each charging schedule also increases. So the travelled path of MC becomes longer and the power of MC uses for charging sensors is reduced. The STCI-TR algorithm takes the MC as a sink node for a collaborative collection. After the charging and the completion of charging, the route planning is carried out again. It reduces the path length from some sensor nodes to sink and MC and the network transmission energy consumption. Therefore, the mobile energy consumption of MC and the stop-wait sensor nodes can be at the same time. The average remaining energy of STCI-TR is higher than that of MCU, BNRS, DPMCS, and VN-MOAC.

6. Conclusions

A charging task coordination algorithm based on the Hamiltonian path for MWRSN is proposed to improve the EUE. This algorithm considers the cooperation of an MC and the next round of charging sensor nodes. In this paper, the MC is considered a mobile sink node to determine the stop position, and the charging task interval of the MC is determined. According to the charging task interval, the next round of the charging sensor node is taken as the stop-wait charging sensor node of the current round, and its stop-wait position is determined. In this way, the next round of charging by the MC node is avoided, and the mobile energy consumption of the MC in the next round of charging tasks is reduced. Simulation results show that the proposed algorithm can improve charging efficiency and network lifetime and reduce network energy consumption and average moving loss per unit time. However, the proposed charging task coordination algorithm needs more control information. The time complexity of the STCI-TR algorithm is still high for the MC and sink nodes. Multiple MCs are not considered in our work. Currently, the proposed method is not suitable for the large-scale network. In future research, collaborative charging between sensors will be considered to improve EUE. In addition, to improve the scalability and adapt to the application of large-scale sensor networks, the multiple sinks and MCs will be considered for cooperative charging. The decomposition of large-scale charging areas is the focus of our future research. The large-scale charging areas will be divided into several small subcharging areas according to the number of MC. An MC is responsible for charging the sensors in a subcharging area and our method in this paper can be used in this scenario. The charging cooperation among multiple MCs and between sensors will be considered in the future research. Another possible direction for future work is the 3D mobile charging of the MWRSN.

Data Availability

The data used to support the findings of this study are available from the corresponding author upon request.

Conflicts of Interest

The authors declare that there are no conflicts of interest.

Authors' Contributions

The authors have read the manuscript and approved its submission.

Acknowledgments

This work was partly supported by the National Natural Science Foundation of China (Grant No. 62002180), Natural Science Foundation of Henan Province (Grant No. 202300410301), General Project of Humanities and Social Sciences Research of Henan Institutions of Higher Learning (Grant No. 2021-ZZJH-262), the Scientific and Technological Project in Henan Province of China (Grant Nos. 202102210362, 212102310481, 222102320369, and 212102210169), the PhD Projects in Nanyang Normal University (Grant No. 18025), the Key Scientific Research Projects of Colleges and Universities in Henan Province (Grant Nos. 21A520033 and 22A520037), the Laboratory Opening Project of Nanyang Normal University (Grant No. SYKF2021029), and Open Project of Key Laboratory of Grain Information Processing and Control of the Ministry of Education (Grant No. KFJJ-2020-114).

References

[1] H. Li, Y. Yang, X. Qiu, Z. Gao, and G. Ma, "Gravitation-based 3-D redeployment schemes for the mobile sensors and sink in gas leakage monitoring," *IEEE Access*, vol. 5, pp. 8545–8558, 2017.

[2] F. Cui, "Deployment and integration of smart sensors with IoT devices detecting fire disasters in huge forest environment," *Computer Communications*, vol. 150, no. 15, pp. 818–827, 2020.

[3] R. Hemalatha, R. Prakash, and C. Sivapragash, "Analysis on energy consumption in smart grid WSN using path operator calculus centrality based HSA-PSO algorithm," *Soft Computing*, vol. 24, no. 14, Article ID 10783, 2020.

[4] Z. Libo, H. Tian, and G. Chunyun, "Wireless multimedia sensor network for rape disease detections," *EURASIP Journal on Wireless Communications and Networking*, vol. 2019, no. 1, p. 159, 2019.

[5] A. B. Hayani and H. Ilhan, "Image transmission over decode and forward based cooperative wireless multimedia sensor networks for Rayleigh fading channels in medical internet of things (MioT) for remote health-care and health communication monitoring," *Journal of Medical Imaging and Health Informatics*, vol. 10, no. 1, pp. 160–168, 2020.

[6] D. P. Kumar, T. Amgoth, and C. S. R. Annavarapu, "Machine learning algorithms for wireless sensor networks: a survey," *Information Fusion*, vol. 49, no. 2019, pp. 1–25, 2019.

[7] A. Kurs, A. Karalis, R. Moffatt, J. D. Joannopoulos, P. Fisher, and M. Soljačić, "Wireless power transfer via strongly coupled magnetic resonances," *Science*, vol. 317, no. 5834, pp. 83–86, 2007.

[8] L. Xie, Y. Shi, Y. T. Hou, W. Lou, H. D. Sherali, and S. F. Midkiff, "On renewable sensor networks with energy transfer: the multi-node case," in *Proceedings of the 9th Ann. IEEE Communications Society Conference Sensor Mesh and Ad Hoc Communications Networking. (SECON)*, pp. 10–18, Seoul, Korea (South), June 2012.

[9] Y. Gu and X. Jia, "Energy consumption detection of sensor nodes in the Internet of things based on modal symmetry algorithm," *Journal of Ambient Intelligence and Humanized Computing*, vol. 6, pp. 1–10, 2021.

[10] J. Q. Zhu, Y. Feng, H. Z. Sun, M. Liu, and Z. N. Zhang, "Energy starvation avoidance mobile charging for wireless rechargeable sensor networks," *Journal of Software*, vol. 29, no. 12, pp. 3868–3885, 2018.

[11] T. N. Nguyen, B.-H. Liu, S.-I. Chu, D.-T. Do, and T. D. Nguyen, "WRSNs: toward an efficient scheduling for mobile chargers," *IEEE Sensors Journal*, vol. 20, no. 12, pp. 6753–6761, 2020.

[12] Z. Wei, C. Xia, X. Yuan et al., "The path planning scheme for joint charging and data collection in WRSNs: a multi-objective optimization method," *Journal of Network and Computer Applications*, vol. 156, Article ID 102565, 2020.

[13] C. Sha, Y. Sun, and R. Malekian, "Research on cost-balanced mobile energy replenishment strategy for wireless rechargeable sensor networks," *IEEE Transactions on Vehicular Technology*, vol. 69, no. 3, pp. 3135–3150, 2020.

[14] C. Zhao, H. Zhang, F. Chen, S. Chen, C. Wu, and T. Wang, "Spatiotemporal charging scheduling in wireless rechargeable sensor networks," *Computer Communications*, vol. 152, pp. 155–170, 2020.

[15] A. Tomar, K. Nitesh, and P. K. Jana, "An efficient scheme for trajectory design of mobile chargers in wireless sensor networks," *Wireless Networks*, vol. 26, no. 2, pp. 897–912, 2020.

[16] P. Zhang, X. Ding, J. Xu, J. Wang, and L. Shi, "Successive interference cancellation based throughput optimization for multi-hop wireless rechargeable sensor networks," *Sensors*, vol. 20, no. 2, p. 327, 2020.

[17] W. Xu, W. Liang, X. Jia, Z. Xu, Z. Li, and Y. Liu, "Maximizing sensor lifetime with the minimal service cost of a mobile charger in wireless sensor networks," *IEEE Transactions on Mobile Computing*, vol. 17, no. 11, pp. 2564–2577, 2018.

[18] R. Zhou, L. Wu, and R. S. Cheng, "Energy-efficiency-oriented charge scheduling and beamforming for a two-tier wireless powered network," *IEEE Internet of Things Journal*, vol. 7, no. 3, pp. 2212–2222, 2020.

[19] A. Tomar and P. K. Jana, "Designing energy efficient traveling paths for multiple mobile chargers in wireless rechargeable sensor networks," in *Proceedings of the 10th International Conference Contemporary Computing (IC3)*, pp. 1–6, Noida, India, August 2017.

[20] A. Tomar, L. Muduli, and P. K. Jana, "A fuzzy logic-based on-demand charging algorithm for wireless rechargeable sensor networks with multiple chargers," *IEEE Transactions on Mobile Computing*, vol. 20, no. 9, pp. 2715–2727, 2021.

[21] S. P. R. Banoth, P. K. Donta, and T. Amgoth, "Dynamic mobile charger scheduling with partial charging strategy for WSNs using deep-Q-networks," *Neural Computing & Applications*, vol. 33, pp. 3868–3885, 2021.

[22] Y. Xiong, G. Chen, M. Lu, X. Wan, M. Wu, and J. She, "A two-phase lifetime-enhancing method for hybrid energy-harvesting wireless sensor network," *IEEE Sensors Journal*, vol. 20, no. 4, pp. 1934–1946, 2020.

[23] C. Wang, J. Li, F. Ye, and Y. Yang, "A mobile data gathering framework for wireless rechargeable sensor networks with vehicle movement costs and capacity constraints," *IEEE Transactions on Computers*, vol. 65, no. 8, pp. 2411–2427, 2016.

[24] X. Li, Q. Tang, and C. Sun, "Energy efficient dispatch strategy for the Dual-functional mobile Sink in wireless rechargeable sensor networks," *Wireless Networks*, vol. 24, no. 3, pp. 671–681, 2018.

[25] Y. Zhang, S. He, and J. Chen, "Near optimal data gathering in rechargeable sensor networks with a mobile Sink," *IEEE Transactions on Mobile Computing*, vol. 16, no. 6, pp. 1718–1729, 2017.

[26] X. Ding, J. H. Han, L. Shi, W. Xia, and Z. C. Wei, "Problem of the dynamic topology architecture of rechargeable wireless sensor networks," *Journal of Communication*, vol. 36, no. 1, pp. 129–141, 2015.

[27] Y. Guo, X. Liu, and C. Chen, "Research on hybrid cooperative charging scheduling schemes in underwater sensor networks," *IEEE Access*, vol. 7, Article ID 156462, 2017.

[28] G. Z. Papadopoulos, A. Mavromatis, A. Gallais, and F. Theoleyre, "CoopStor: a cooperative reliable and efficient data collection protocol in fault and delay tolerant wireless networks," *Wireless Networks*, vol. 27, no. 1, pp. 367–381, 2020.

[29] J. Zhao, X. Dai, and X. Wang, "Scheduling with collaborative mobile chargers Inter-WSNs," *International Journal of Distributed Sensor Networks*, vol. 11, no. 5, Article ID 921397, 2015.

[30] S. Zhang, J. Wu, and S. Lu, "Collaborative mobile charging," *IEEE Transactions on Computers*, vol. 64, no. 3, pp. 654–667, 2015.

[31] T. Liu, B. Wu, H. Wu, and J. Peng, "Low-cost collaborative mobile charging for large-scale wireless sensor networks," *IEEE Transactions on Mobile Computing*, vol. 16, no. 8, pp. 2213–2227, 2017.

[32] C. Lin, J. Zhou, C. Guo, H. Song, G. Wu, and M. S. Obaidat, "TSCA: a temporal-spatial real-time charging scheduling algorithm for on-demand architecture in wireless rechargeable sensor networks," *IEEE Transactions on Mobile Computing*, vol. 17, no. 1, pp. 211–224, 2018.

[33] M. Tian, W. Jiao, and J. Liu, "The charging strategy of mobile charging vehicles in wireless rechargeable sensor networks with heterogeneous sensors," *IEEE Access*, vol. 8, Article ID 73110, 2020.

[34] Y. Wang, X. Zhang, C. X. Zhao, Q. Fang, and S. C. Ai, "Directional charging schedule scheme based on charging utility maximization for wireless rechargeable sensor network," *Journal of Electronics and Information Technology*, vol. 43, no. 5, pp. 1331–1338, 2021.

[35] N. Gharaei, Y. D. Al-Otaibi, S. Rahim, H. J. Alyamani, N. A. K. K. Khani, and S. J. Malebary, "Broker-based nodes recharging scheme for surveillance wireless rechargeable sensor networks," *IEEE Sensors Journal*, vol. 21, no. 7, pp. 9242–9249, 2021.

[36] Z. W. Lü, Z. C. Wei, J. H. Han, R. H. Sun, and C. K. Xia, "A mobile charging and data collecting algorithm based on multi-objective optimization," *Journal of Electronics and Information Technology*, vol. 41, no. 8, pp. 1877–1884, 2019.

[37] Z. Sun and J. H. Reif, "On finding energy-minimizing paths on terrains," *IEEE Transactions on Robotics*, vol. 21, no. 1, pp. 102–114, 2005.

[38] D. K. Sah, K. Cengiz, P. K. Donta, V. N. Inukollu, and T. Amgoth, "EDGF: empirical dataset generation framework for wireless sensor networks," *Computer Communications*, vol. 180, pp. 48–56, 2021.

[39] W. B. Heinzelman, A. P. Chandrakasan, and H. Balakrishnan, "An application-specific protocol architecture for wireless microsensor networks," *IEEE Transactions on Wireless Communications*, vol. 1, no. 4, pp. 660–670, 2002.

[40] J. Yi, "A piezo-sensor-based "smart tire" system for mobile robots and vehicles," *IEEE/ASME Transactions on Mechatronics*, vol. 13, no. 1, pp. 95–103, 2008.